Journal of Industrial and Management Optimization

https://www.aimspress.com/journal/jimo

JIMO, 22(8): 3562–3604.
DOI:10.3934/jimo.2026130
Received: 08 May 2026
Revised: 13 June 2026
Accepted: 22 June 2026
Published: 06 July 2026

Research article

Green electric vehicle battery recycling network design under supply chain disruptions: a 4PL-based approach with combinatorial auction-based winner determination

Yingfu Zhang[1], **Xuefeng Wang**[1,*], **Mingqiang Yin**[1,2,3,*], **Guodong Liang**[1], **Xiaohu Qian**[4] **and Chunxi Han**[1]

[1] School of Information and Control Engineering, Liaoning Petrochemical University, Fushun, Liaoning, 113001, China

[2] Chongqing Rongyuan Science Technologies Co., Ltd., Chongqing 400039, China

[3] Chongqing Jiaotong University, Chongqing 400074, China

[4] Research Institute of Business Analytics & Supply Chain Management, College of Management, Shenzhen University, Shenzhen 518060, China

* **Correspondence:** Email:xuefeng183305@163.com, yinmingqiang2387@sina.com.

Abstract: With the rapid development of electric vehicles, a large number of end-of-life power batteries are entering the recycling stage. Under carbon emission constraints and uncertain disruption risks, the construction of an efficient, low-carbon, and resilient recycling network has become a critical issue. From a fourth-party logistics perspective, this study investigated an electric vehicle battery (EVB) recycling network design problem that integrates internal recycling operations with external resource collaboration, and a combinatorial auction framework with an embedded winner determination mechanism was introduced to enable dynamic allocation of external recycling capacity. On this basis, a two-stage stochastic programming model incorporating carbon emission constraints and disruption scenarios was developed to optimize network configuration and resource allocation decisions. To address the computational challenges of large-scale problems, a hybrid algorithm that integrates scenario reduction and Lagrangian relaxation based on the progressive hedging algorithm was proposed to improve solution efficiency and obtain high-quality solutions. Numerical experiments and validation were conducted based on a real-world case. The results indicate that the proposed SR-LR algorithm consistently achieves optimality gaps below 0.01% and obtains solutions within 3–37 seconds across all test instances. By comparison, CPLEX requires from 12.9 minutes to 2.35 hours for solvable instances and is unable to solve several large-scale scenarios within acceptable computational limits. These findings provide useful insights for planning and decision-making for EVB recycling networks in a low-carbon context.

Keywords: electric vehicle battery recycling; network design; combinatorial auction; winner determination; disruption uncertainty; carbon emission constraints
Mathematics Subject Classification: 90B06, 90C15

1. Introduction

As electric vehicle adoption continues to accelerate, an increasing volume of batteries is reaching the end-of-life phase, making their recovery and secondary utilization a critical issue. Establishing an effective recycling network not only facilitates the circular use of valuable metal resources, but also helps mitigate environmental impacts and supports sustainable development. Xu et al. [1] indicated that the continuous growth in the global electric vehicle stock will drive the scale of retired batteries to accumulate exponentially, and the recycling potential of critical metal resources will be progressively enhanced with the increase in retired volumes. Under such a background, supply chain network design, as a typical approach for facility location and logistics system planning, has been widely applied to electric vehicle battery (EVB) recycling networks. Govindan et al. [2] demonstrated that network design enables coordinated decision-making for facility layout and logistics routing from a system-wide perspective. Compared with the vehicle routing problem, which primarily focuses on transportation route optimization, stronger global optimization capability at the strategic level can be achieved, thereby effectively reducing system costs and improving operational efficiency.

However, traditional network design is generally developed under deterministic environments, and such an assumption makes it difficult to capture the uncertainty and disruption risks that are widely present in recycling systems. Gurtu and Johny [3] indicated that supply chain systems are highly susceptible to external environments and human-related factors during practical operations. Natural disasters, extreme weather conditions, equipment failures, and human disruptions may lead to supply chain interruptions and can impose significant impacts on system performance. To address such issues, several studies have introduced external logistics service providers to enhance system flexibility and adaptability. Among these studies, Li and Chen [4] examined the design of a reverse logistics network in the presence of disruption risks by incorporating third-party logistics (3PL) service providers; their findings indicate that leveraging external logistics resources can enhance system performance under uncertainty. However, such approaches typically rely on single or limited logistics providers, and systematic coordination of multi-source logistics resources is insufficiently addressed. To enhance the adaptability of recycling networks in complex environments, Huang et al. [5] integrated a fourth-party logistics (4PL) mechanism into a network design model. As an integrator and coordinator within supply chains, 4PL enables unified management and scheduling of multiple logistics resources, thereby improving system coordination efficiency and responsiveness. Yin et al. [6] indicated that the introduction of 4PL into network design can effectively integrate existing logistics resources, thereby alleviating the adverse impacts caused by facility disruptions or demand fluctuations to a certain extent. Furthermore, Yin et al. [7] extended the 4PL mechanism to the design of EVB recycling networks, and verified its applicability in complex and uncertain environments from the perspectives of sustainability and resilience. Moreover, traditional fixed contractual arrangements commonly adopted in logistics and recycling systems usually require service capacities, cooperation relationships, and resource commitments to be determined in advance. Although such arrangements may perform adequately under stable operating conditions, they often lack flexibility when disruption events, demand fluctuations, or sudden capacity shortages occur. Caplice and Sheffi [8] demonstrated that bundled bidding in transportation procurement auctions can significantly improve allocation efficiency compared with traditional fixed contracting approaches. Furthermore, Qian et al. [9] integrated a 4PL coordination framework with a combinatorial reverse auction and winner determination (WD) mechanism under disruption risks. Their study showed that allowing logistics service providers to submit package bids enables the decision maker to exploit complementarities, synergies, and economies of scale among different service combinations, thereby improving resource allocation flexibility and system adaptability. Therefore, compared with fixed contractual arrangements, auction-based allocation mechanisms provide greater flexibility and adaptability for disruption-prone logistics and recycling networks.

To address the aforementioned issues, recent studies have introduced the WD mechanism of combinatorial auction to enable flexible allocation of external resources. Combinatorial auctions allow service providers to submit bids on bundles of logistics tasks or routes, through which complementarities and synergistic effects among resources can be explicitly characterized, and overall optimal allocation can be achieved via the WD process. Buer and Haass [10] embedded the combinatorial auction mechanism into supply chain network design, and significant improvements in resource allocation efficiency were achieved under collaborative planning environments characterized by multiple decision-makers and private information. Furthermore, Wang et al. [11] applied the integration of network design and combinatorial auction approaches to EVB recycling systems. Optional external 3PL resources were introduced in addition to internal logistics resources, and optimization-based selection was conducted through auction mechanisms, thereby effectively addressing disruption risks and enhancing system flexibility. However, primary attention in such studies has been paid to economic cost and system resilience, whereas environmental impacts during the recycling process have received insufficient consideration. Driven by the carbon neutrality targets and green development principles, carbon emissions have become a critical issue in supply chain optimization research. The recycling process of EVBs involves multi-echelon transportation and multi-stage processing, and significant carbon emissions are generated during transportation, dismantling, and remanufacturing stages. Wang et al. [12] indicated that optimization solely based on economic cost may lead to the preferential selection of high-emission routes or energy-intensive processing methods, thereby weakening the environmental benefits of recycling systems. Therefore, the incorporation of carbon emissions into recycling network design models, and the realization of coordinated optimization between economic and environmental objectives, are of substantial theoretical and practical significance. Although carbon emission factors have been incorporated into EVB recycling network design by Liao et al. [13] and Wang et al. [14], existing studies have not yet integrated carbon emission constraints with combinatorial auction mechanisms under the perspective of 4PL, nor has such integration been systematically investigated within uncertain environments.

Based on the above analysis, this study focuses on how enterprises conduct EVB recycling network design and resource allocation decisions under the coexistence of uncertain disruption environments and green low-carbon development objectives. Different from prior studies that primarily emphasize economic cost or single network structure optimization, a comprehensive optimization framework is developed under the system coordination perspective of 4PL, in which carbon emissions are treated as one of the core decision dimensions, and self-built recycling networks, external resource collaboration, and environmental constraints are integrated. Specifically, considering the heterogeneity of multi-source external recycling resources in terms of service capacity and cost structures, the WD mechanism in combinatorial auction is innovatively embedded into the recycling network design process. Through such integration, flexible selection of external recycling schemes can be achieved via market-oriented mechanisms when internal recycling capacity is limited or disrupted, thereby improving resource allocation efficiency and system flexibility. On this basis, a two-stage stochastic programming (TSSP) approach is proposed, in which facility location and reinforcement decisions, logistics routing configurations, and external resource selection are jointly optimized. Carbon emission accounting and constraint mechanisms are incorporated to explicitly characterize environmental impacts during transportation and processing stages, enabling coordinated trade-offs among economic cost, system resilience, and carbon emissions. Meanwhile, to mitigate the computational complexity arising from multi-scenario stochastic optimization, a hybrid scenario reduction and Lagrangian relaxation (SR-LR) algorithm is designed to improve solution efficiency. Validation of the proposed model and approach is conducted through a real-world case study, from which managerial insights are further derived under a green low-carbon context.

The main contributions of this study can be summarized as follows:

(1) A two-stage stochastic programming model is developed for EVB recycling network design under the joint consideration of carbon-emission constraints and disruption risks. Unlike existing carbon-constrained recycling network studies that generally assume stable operating conditions, the proposed model explicitly incorporates facility disruption scenarios and reinforcement decisions, enabling the simultaneous consideration of environmental and resilience objectives.

(2) An outsourcing structure based on combinatorial auctions is integrated into the EVB recycling network through the WD mechanism. This enables the coordinated selection of external recyclers and allocation of recycling tasks, thereby enhancing network flexibility under capacity shortages and disruption conditions.

(3) Considering that the introduction of uncertain disruption scenarios leads to a rapid expansion of model scale and makes it difficult for traditional commercial solvers such as IBM ILOG CPLEX Optimization Studio (CPLEX) to obtain feasible solutions within reasonable time, a hybrid algorithm that integrates scenario reduction and Lagrangian relaxation, referred to as SR-LR, is designed to effectively reduce computational complexity and significantly improve solution efficiency.

(4) Numerical experiments based on a real-world case are conducted for performance assessment of the proposed model and algorithm, thereby offering practical decision support for EVB recycling network planning and optimization within a green and low-carbon context.

The remainder of this paper is organized as follows: Section 2 reviews the literature on EVB recycling networks, 4PL systems, combinatorial auctions, and low-carbon constraints, and identifies research gaps. Section 3 introduces the problem setting, notation, and a TSSP model incorporating the WD mechanism, facility reinforcement, and carbon constraints. Section 4 develops a hybrid SR-LR algorithm combining scenario reduction and Lagrangian relaxation to improve computational efficiency under large-scale scenarios. Section 5 presents numerical results based on a real-world case and sensitivity analyses. Section 6 discusses managerial and policy implications. Section 7 concludes the paper and outlines future research directions.

2. Literature review

To systematically review the research stream of EVB recycling network design, related studies are classified from different research perspectives. Specifically, Section 2.1 reviews EVB recycling network design problems, with a focus on deterministic and stochastic modeling approaches; Section 2.2 summarizes the application of 4PL in supply chain networks; Section 2.3 synthesizes research progress on combinatorial auction mechanisms in logistics resource allocation; and Section 2.4 further analyzes EVB recycling network optimization studies that incorporate carbon emission factors. In addition, to more clearly distinguish the contributions of the present study from those of closely related research, a comparative summary of the relevant literature is provided in Table 1.

Table 1. Summary of relevant literature.

References	RN	4PL	CA	D	FR	CR	ER	C	Solution algorithm	Real-world case study
Li et al. [4]				✓					CPLEX	None
Huang et al. [5]		✓							AL, Greedy heuristic, CPLEX	HP (Shanghai, China)
Yin et al.		✓		✓					SAA, SR, DDLR, CPLEX	Logistics firm (Shenzhen, China)
Yin et al. [7]	✓	✓		✓	✓	✓	✓		SRDBH, CPLEX	JMC & DFM (Jiangxi, China)
Caplice et al. [8]			✓						MIP, CPLEX	Retail firms (USA)
Wang et al. [11]	✓	✓	✓	✓	✓	✓	✓		SRDA, LR, CPLEX	JMC & DFM (Jiangxi, China)
Wang et al. [12]								✓	GA	Changan Auto (Chongqing, China)
Harper et al. [15]	✓								Review	None
Gaines et al. [16]	✓								None	None
Dunn et al. [17]									None	None
Govindan et al. [18]									Review	None
Melo et al. [19]									Review	None
Farahani et al [20]									Review	None
ReVelle and Eiselt [21]									Review	None
Min and Ko [22]									GA	None
Pishvaee et al. [23]									ABD	Medical manufacturer (Iran)
Casals et al. [24]									Equivalent circuit model	Sunbat project (Spain)
Tan et al. [25]									None	None
Snyder [26]									Review	None
Yan et al. [27]	✓							✓	GA, FCCP	Region T (China)
Rosenberg et al. [28]	✓						✓		Two-stage SP, BD, CPLEX	Auto network (Germany)
Win [29]		✓							None	Beverage firms (NZ & AU)
Hingley et al. [30]		✓							None	Retail chain (UK)
Tao [31]		✓				✓			CG, GSH, CPLEX	None
Vries and Vohra [32]			✓						Review	None
Li et al. [33]			✓						SRO, MILP, Gurobi/CPLEX	None
Triki et al. [34]			✓			✓			MILP, CPLEX	None
Bektaş and Laporte [35]								✓	MILP, CPLEX	None
Chaabane et al. [36]								✓	MILP, LINGO	Aluminum supply chain
Wang et al. [37]									None	None
Li et al. [38]	✓							✓	LR heuristic, MINLP	JMEV & DFEV (Jiangxi, China)
He et al. [39]	✓							✓	FCCP, LINGO	Yangtze River Delta (China)
This study	✓	✓	✓	✓	✓	✓	✓	✓	SR-LR, CPLEX	JMC & DFM (Jiangxi, China)

*Note: RN = EVB recycling network; 4PL = fourth-party logistics coordination; CA = combinatorial auction; D = disruption modeling; FR = facility reinforcement; CR = capacity reservation; ER = external resource allocation; C = carbon constraint.

AL = Approximation linearization; GA = Genetic algorithm; MIP/MILP = Mixed integer (nonlinear) programming; SP = Stochastic programming; BD = Benders decomposition; CG = Column generation; SRO = Sample robust optimization; FCCP = Fuzzy chance-constrained programming; LR = Lagrangian relaxation; ABD = Accelerated Benders decomposition; SR = Scenario reduction; Review = Review article.

JMC = Jiangling Motors; DFM = Dongfeng Motor; JMEV = Jiangling EV; DFEV = Dongfeng EV; NZ = New Zealand; AU = Australia.

2.1. *Review of EVB recycling network design*

As the electric vehicle industry continues to expand, an increasing number of batteries are reaching the end-of-life phase, leading to a steady growth in the volume of retired EVBs [15]. EVBs contain valuable metals, including nickel, lithium, and cobalt, while potential environmental risks are also associated with such batteries. Therefore, the construction of efficient recycling and reutilization systems is of great importance for resource circularity and environmental protection [16, 17].

Under such a background, supply chain network design approaches have been widely applied to EVB recycling systems. A typical recycling network generally consists of multiple echelons, including collection points, inspection centers, dismantling centers, and remanufacturing or reuse nodes [18]. Network design problems involve facility location, capacity allocation, and logistics routing decisions, and the core objective is defined as achieving system-wide optimality under demand satisfaction and operational constraints [19, 20].

From the perspective of modeling approaches, existing studies are generally divided into two groups. The first group relies on deterministic assumptions, under which mixed-integer programming models are typically adopted for facility location and routing optimization [19, 21]. Related studies have been further extended to multiple products, multiple stages, and closed-loop supply chain systems [22, 23]. In EVB recycling research, several studies consider different battery processing pathways and cascade utilization strategies [24, 25], while deterministic environments are still predominantly assumed.

The second category incorporates uncertainty and disruption risks to enhance system adaptability in complex environments. Representative approaches include TSSP and robust optimization [23, 26]. In recent years, factors such as demand fluctuations and facility disruptions have been incorporated into recycling network design, and system resilience has been improved through scenario analysis and redundancy allocation [4]. In the EVB recycling context, uncertainty has been progressively considered in network design; for example, stochastic programming methods have been applied to characterize uncertainties in battery quantity and quality, and dynamic network frameworks have been adopted to analyze recycling and processing decisions under uncertain environments [27, 28]. However, such studies have primarily focused on internal network structure adjustments, whereas limited attention has been paid to the coordinated utilization and dynamic allocation of external logistics resources.

2.2. *Application of 4PL in supply chain network design*

4PL, as an integrator and coordinator in supply chains, was first proposed by Accenture. Different from 3PL, which primarily provides specific services such as transportation and warehousing, 4PL focuses on integrating and centrally managing multiple logistics resources [29]. Through the coordination of multiple logistics service providers, system-level efficiency and responsiveness can be improved [30].

In supply chain network design research, existing studies have incorporated 4PL mechanisms into traditional logistics systems, and unified scheduling of multi-source resources has been achieved to reduce costs and improve service levels [31]. However, primary attention in such studies has been directed toward forward supply chains, whereas reverse logistics systems have received relatively limited consideration.

In recent years, 4PL has been gradually applied to recycling and reverse logistics network design. Huang et al. [5] introduced a 4PL coordination mechanism into the network design framework to achieve unified management of multiple logistics resources; Yin et al. [6] further indicated that integration of existing logistics resources can be facilitated by 4PL, thereby alleviating the impacts of uncertainty on system operations. Furthermore, Yin et al. [7] applied 4PL to EVB recycling networks, and effectiveness was verified from the perspectives of sustainability and resilience.

Although significant advantages of 4PL in resource integration have been demonstrated, existing studies have primarily emphasized coordination functions, whereas limited attention has been paid to specific configuration strategies of multi-source logistics resources. In complex environments characterized by multiple routes and service combinations, reliance on fixed partnerships or simple allocation mechanisms makes it difficult to capture synergistic effects among different resource combinations, thereby restricting system flexibility under uncertain conditions.

2.3. Application of combinatorial auction mechanisms in supply chain and recycling network design

Combinatorial auction allows bidders to submit joint bids on bundles of resources, through which complementary or substitutive relationships among resources can be expressed. The core problem is defined as the WD problem, and such a problem has been proven to be NP-hard [32].

In supply chain and logistics systems, combinatorial auctions have been widely applied to transportation task allocation and collaborative optimization problems. Existing studies have shown that, by allowing logistics service providers to bid on multiple routes or tasks in combination, resource allocation efficiency can be significantly improved, and system costs can be reduced [8, 33, 34]. Such a mechanism enables explicit characterization of synergistic effects among resources, and superior performance can be achieved compared with traditional item-by-item allocation approaches.

In recent years, combinatorial auctions have been gradually introduced into reverse logistics and recycling network design. As an example, Wang et al. [11] applied this mechanism in EVB recycling networks, and dynamic allocation of external resources was realized via the WD process, thereby improving system adaptability under uncertain environments.

However, existing studies have primarily focused on the optimization of economic cost or system efficiency, whereas environmental factors, such as carbon emissions, have received relatively limited consideration. Under the context of green supply chains, incorporation of environmental impacts into resource allocation processes remains an issue that requires further investigation.

2.4. EVB recycling network optimization considering carbon emissions

Driven by the carbon neutrality targets and green development principles, carbon emissions have become an important research direction in supply chain network design. Existing studies have typically incorporated carbon emissions into optimization models, and impacts on network design have been characterized through carbon constraints or carbon costs [35, 36].

In EVB recycling research, carbon emission factors are increasingly integrated into network design frameworks. Wang et al. [37] indicated that optimization based solely on cost minimization may result in the preferential selection of high-emission routes; Wang et al. [12], Li et al. [38], and He et al. [39] achieved coordinated optimization of economic and environmental objectives by introducing carbon constraints or carbon costs.

Although carbon emission factors have been considered in end-of-life EVBs recycling networks, existing studies have mainly focused on traditional network structures or single decision dimensions, and limited attention has been paid to the integration with 4PL coordination mechanisms, combinatorial auction-based resource allocation, and uncertainty-induced disruption risks. Under the context of multi-source logistics and complex environments, the synergistic relationship between carbon emissions and resource allocation decisions remains insufficiently explored.

In summary, existing studies have achieved significant progress in EVB recycling network design, uncertainty modeling, 4PL-based resource coordination, and combinatorial auction mechanisms, and carbon emission factors have been gradually incorporated into optimization frameworks. However, several limitations remain. Current literature has primarily focused on internal network structure optimization or single decision dimensions, and systematic characterization of coordinated configuration of multi-source logistics resources is lacking. Although resource integration can be achieved by 4PL, deep integration with specific resource allocation mechanisms, such as combinatorial auction, remains limited, and synergistic effects among different resource combinations cannot be fully captured. Meanwhile, existing studies on combinatorial auctions have mainly emphasized cost or efficiency optimization, whereas environmental factors such as carbon emissions have received insufficient attention. Under the context of uncertainty and disruption risks, the above elements have not yet been comprehensively considered within a unified framework. Therefore, in EVB recycling network design, effective integration of 4PL coordination mechanisms, combinatorial auction-based resource allocation, and carbon emission decision-making under uncertain environments, so that coordinated optimization of economic performance, environmental impact, and system resilience can be achieved, remains an important issue that requires further investigation.

3. Problem description and model formulation

Under carbon emission constraints and uncertain disruption risks, the EVB recycling network design problem is systematically studied from a 4PL coordination perspective in this section. Internal recycling network operations and external resource collaboration driven by combinatorial auction are integrated into a unified framework, and a TSSP approach is adopted to characterize joint strategic and operational decision-making under uncertain environments. Section 3.1 describes the problem setting and logical framework of the recycling network; Section 3.2 introduces the model sets, parameters, and decision variables; and Section 3.3 develops a TSSP formulation incorporating the WD mechanism, multi-level facility reinforcement strategies, and carbon emission constraints, and presents the complete mathematical model.

3.1. Problem description

Driven by the rapid expansion of the electric vehicle industry, increasing volumes of end-of-life power batteries are continuously entering recycling systems, making the development of an efficient, low-carbon, and disruption-resilient recycling network an important research issue in supply chain management. Based on this background, an EVB recycling network design problem is investigated from the perspective of 4PL coordination, in which an integrated framework is developed by combining a self-built recycling network with external recycling resource collaboration. Under uncertain disruption environments, the combinatorial auction mechanism and carbon emission factors are incorporated into a unified optimization framework, as shown in Figure 1.

The recycling network considered in this study is composed of collection regions, collection centers, remanufacturing centers, and disposal centers. End-of-life batteries generated in each collection region are required to be collected in a timely manner and transported to collection centers for centralized processing. At collection centers, batteries are first dismantled into battery cells and then classified according to their performance conditions. A portion of batteries possesses reuse value, in which recoverable cells and non-recoverable cells are separated. Recoverable components are transported to remanufacturing centers for remanufacturing processes, while non-recoverable components are treated as waste and transported to disposal centers. For batteries without reuse value, waste is directly generated after processing at collection centers and then transported to disposal centers.

In terms of logistics operations, transportation tasks in the self-built network are undertaken by multiple 3PL service providers, covering key transportation links including collection regions to collection centers, collection centers to remanufacturing and disposal centers, and remanufacturing centers to disposal centers. To enhance system flexibility and redundancy, multiple candidate logistics schemes are considered for each transportation route to cope with demand fluctuations and potential disruptions. However, in practical operations, collection centers, remanufacturing centers, and disposal centers may experience disruptions due to facility failures, natural disasters, or other uncertainties, which may lead to insufficient processing capacity or even partial system failure. To improve system adaptability under disruption scenarios, external recyclers are introduced as complementary resources on the basis of the self-built network. When internal network capacity is insufficient to satisfy recycling demand, part of the recycling tasks can be outsourced to external recyclers. External recyclers participate in the recycling system through combinatorial bids, and the optimal outsourcing scheme is determined by the WD mechanism. The WD decision is made at the strategic planning stage and determines the set of external recyclers that can participate in the recycling network. After disruption realizations become known, the actual recycling quantities assigned to the selected external recyclers are adjusted according to scenario-specific operational requirements. From the perspective of the focal enterprise, the decision process concerns the selection of external recyclers and the allocation of recycling quantities. The subsequent operational activities undertaken by the selected recyclers are managed through their own recycling channels. Accordingly, the carbon accounting boundary considered in this study is limited to transportation and processing activities within the self-built recycling network that are directly managed by the focal enterprise.

To achieve efficient allocation of external resources, the combinatorial auction mechanism is adopted for external recycler selection. Each external recycler is allowed to submit combinatorial service bids for multiple recycling tasks or transportation demands, and a unified evaluation is conducted through a WD mechanism to select the optimal combination of service schemes with minimum cost. In this process, 4PL acts as the system coordinator to integrate and schedule both self-built networks and external resources, thereby improving the coordination efficiency of multi-source logistics resources. Furthermore, facility reinforcement and capacity reservation strategies are introduced at the network design stage to enhance system resilience. Through differentiated reinforcement strategies for different types of facilities, disruption probabilities can be reduced or disruption impacts can be mitigated. Meanwhile, reserved processing capacity ensures that facilities can maintain basic operational capability under disruption scenarios, thereby improving overall system stability. Under the background of green and low-carbon development, carbon emissions are considered an important factor in recycling network design. System carbon emissions mainly stem from transportation activities as well as energy consumption during dismantling, remanufacturing, and disposal processes. By introducing carbon emission accounting mechanisms and carbon cost constraints, the model is able to control environmental impacts while optimizing economic performance, thereby achieving a comprehensive trade-off among cost, resilience, and carbon emissions.

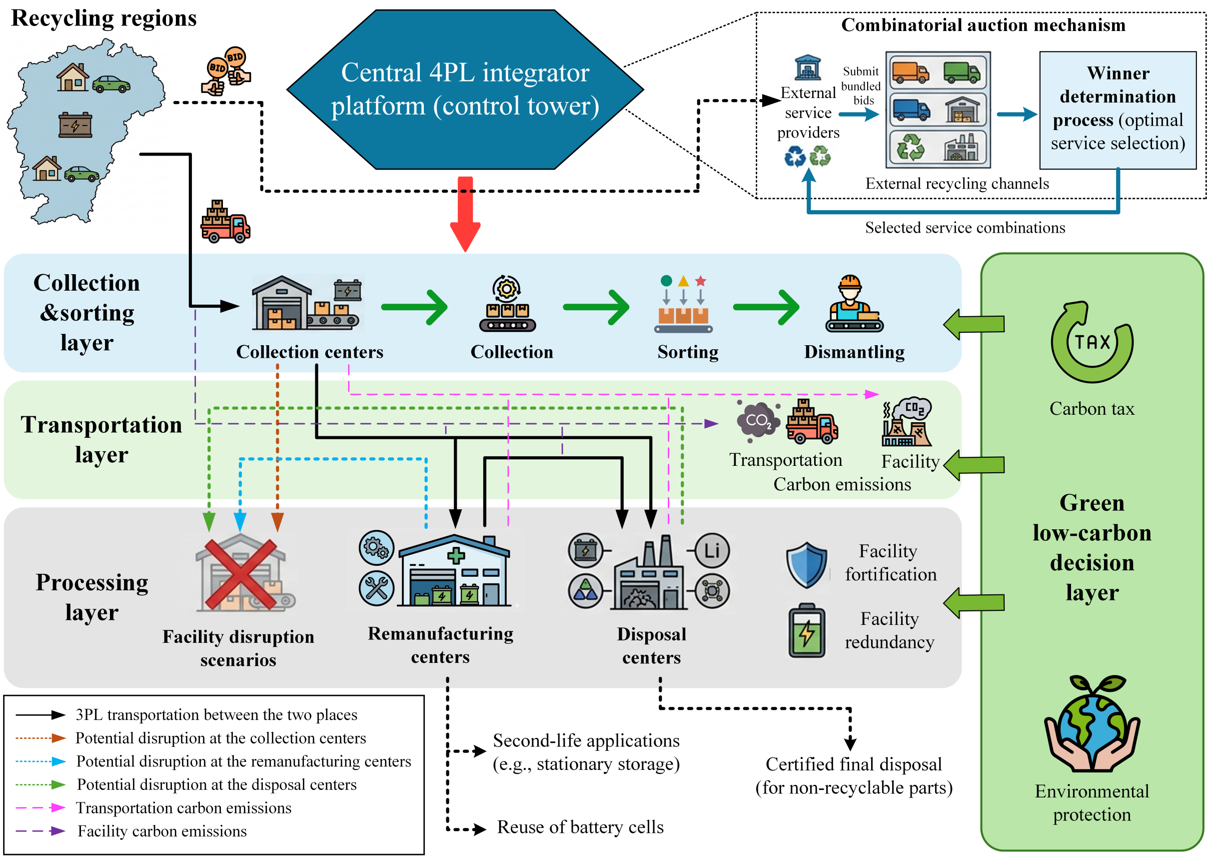

Figure 1. Sustainable EVB recycling network under the 4PL framework.

Considering that facility disruptions may occur under different operating environments, uncertainty is represented in this study through a finite set of disruption scenarios. Each scenario corresponds to a specific disruption realization and is associated with a known occurrence probability estimated from historical information and expert judgment. Under this scenario-based representation of uncertainty, strategic decisions such as facility location, reinforcement, and capacity reservation must be determined before the actual disruption scenario is observed, whereas operational decisions, including scenario-dependent transportation and recycling quantity allocations, are determined after the disruption realization becomes known. Therefore, a two-stage stochastic programming framework is adopted to explicitly capture the sequential nature of decision-making under disruption uncertainty, where strategic network design decisions are made before disruption realization and operational adjustment decisions are implemented after the disruption scenario is observed. In summary, this study aims to construct an EVB recycling network that simultaneously considers economic efficiency, environmental sustainability, and system resilience by jointly optimizing facility location and reinforcement decisions, capacity reservation strategies, 3PL configuration, and external resource selection based on combinatorial auctions under uncertain disruption environments.

3.2. Notation description

Table 2. Model notation.

Sets	**Definition**
D	Collection regions
C	Candidate collection centers
R	Candidate remanufacturing centers
W	Candidate disposal centers
Θ	Disruption scenarios
K	The k-th 3PL provider between two locations
H	External recyclers
I_h	Bid bundles of external recyclers
Z	Total number of bid bundles allowed for external recyclers, where $Z_{\min}$ and $Z_{\max}$ denote the minimum and maximum values, respectively
L	Battery classification level indicating its recyclability; $L \in \{1, 2, 3\}$
E	Reinforcement level, $E \in \{0, 1, 2\}$, where 0 indicates no reinforcement, and 1 and 2 represent first-level and second-level reinforcement, respectively
Parameters	
ϑ	Penalty cost for unrecovered batteries per unit
$X_{\max}$	Upper bound of reservation and reinforcement costs
Num	Number of cells in each battery pack
$\hat{\omega}$	Battery pack weight
ω	Battery cell weight
m_l	Unit recycling cost for level-l batteries
α_l	Proportion of level-l batteries
φ_l	Proportion of battery cell dismantling waste at level l
f_c, f_r, f_w	Construction cost for collection center c, remanufacturing center r, and disposal center w
$\hat{f}_{ce}, \hat{f}_{re}, \hat{f}_{we}$	Reinforcement cost of centers under different reinforcement levels
$\tilde{f}_c, \tilde{f}_r, \tilde{f}_w$	Unit reservation cost of centers
$f_{dck}, f_{crk}, f_{cwk}, f_{rwk}$	3PL setup cost between two locations

Continued on next page

Parameters	
$\lambda_{ce}, \lambda_{re}, \lambda_{we}$	Percentage of retained processing capacity of centers under reinforcement level e
V_c, V_r, V_w	Upper bound of processing capacity at centers
M_c, M_r, M_w	Upper bound of reservation capacity of centers
j_c, j_r, j_w	Unit processing cost for centers
$s_{dc}, s_{cr}, s_{cw}, s_{rw}$	Distance between two locations
$t_{dck}, t_{crk}, t_{cwk}, t_{rwk}$	Unit transportation cost of 3PL
ξ_d	Recycling demand of end-of-life batteries
$g^1_{dck}, g^2_{crk}, g^3_{cwk}, g^3_{rwk}$	Maximum transportation capacity across facility pairs for the k-th 3PL provider. Superscripts 1, 2, and 3 denote battery packs, battery cells, and the weight of waste converted from battery cells, respectively
p_θ	Probability of each disruption scenario
$q_{c\theta}$	Disruption of collection center c under scenario θ; $q_{c\theta} = 1$ if disrupted, and 0 otherwise
$q_{r\theta}$	Disruption of remanufacturing center r under scenario θ; $q_{r\theta} = 1$ if disrupted, and 0 otherwise
$q_{w\theta}$	Disruption of disposal center w under scenario θ; $q_{w\theta} = 1$ if disrupted, and 0 otherwise
v_h	External recycler management cost
b_{hi}	Bidding price per unit for the i-th bid bundle offered by external recycler h
A_{dhi}	Auxiliary coefficient matrix for the combinatorial auction
UP_{hi}	Maximum number of batteries in the i-th bid bundle of external recyclers
P_{ct}	Unit carbon tax rate
$P_{\text{transport}}$	Unit carbon emissions from transportation
$P_{\text{process},c}, P_{\text{process},r}, P_{\text{process},w}$	Unit carbon emissions from processing at centers
UB_{carbon}	Upper bound of total carbon emissions

Continued on next page

Decision variables	
$v^1_{dck\theta}, v^2_{crkl\theta}, v^3_{cwk\theta}, v^3_{rwk\theta}, v^1_{hi\theta}, v^{rest}_{d\theta}$	These variables respectively represent: (1) battery packs transported by the k-th 3PL provider; (2) level-$l \in 1,2$ battery cells transported by the k-th 3PL provider; (3) waste weight converted from non-recyclable level-$l \in 3$ battery cells; (4) waste weight derived from non-recyclable cells originally in level-$l \in 1,2$ batteries; (5) batteries included in the i-th bid bundle of external recycler h; and (6) unrecovered end-of-life EVBs in collection region d. Superscripts 1, 2, and 3 denote battery packs, battery cells, and waste weight converted from battery cells, respectively
x_{ce}, x_{re}, x_{we}	Selection of recycling, remanufacturing, and disposal centers under reinforcement level e
$y_{dck}, y_{crk}, y_{cwk}, y_{rwk}$	Selection of the k-th 3PL provider between facility pairs
m_c, m_r, m_w	Reserved capacity for recycling, remanufacturing, and disposal centers
z_{hi}	Selection of external recyclers in the combinatorial auction
T_θ	Auxiliary decision variable representing the total carbon emissions of the entire recycling network under scenario θ
$T_{transport,\theta}, T_{process,\theta}$	Auxiliary decision variables representing transportation-related carbon emissions and facility processing carbon emissions under scenario θ, respectively

3.3. Model formulation

Building on the problem description and notation, this section formulates a TSSP model that accounts for carbon emission constraints and facility disruption scenarios. The combinatorial auction with WD mechanism, together with facility location and reinforcement decisions, capacity reservation, and logistics routing selection, are incorporated within a unified optimization framework. The objective is to jointly minimize total recycling network cost while controlling carbon emissions and enhancing system resilience under uncertainty. The first-stage stochastic programming (TSSP1) model and the second-stage stochastic programming (TSSP2) model are given as follows:
(TSSP1)

$$\begin{aligned}
\min & \sum_{c\in C}\sum_{e\in E}\left(f_c+\hat{f}_{ce}\right)x_{ce}+\sum_{r\in R}\sum_{e\in E}\left(f_r+\hat{f}_{re}\right)x_{re}+\sum_{w\in W}\sum_{e\in E}\left(f_w+\hat{f}_{we}\right)x_{we}+\\
& \sum_{c\in C}\tilde{f}_c m_c+\sum_{r\in R}\tilde{f}_r m_r+\sum_{w\in W}\tilde{f}_w m_w+\\
& \sum_{d\in D}\sum_{c\in C}\sum_{k\in K_{dc}} f_{dck}y_{dck}+\sum_{c\in C}\sum_{r\in R}\sum_{k\in K_{cr}} f_{crk}y_{crk}+\sum_{c\in C}\sum_{w\in W}\sum_{k\in K_{cw}} f_{cwk}y_{cwk}+\sum_{r\in R}\sum_{w\in W}\sum_{k\in K_{rw}} f_{rwk}y_{rwk}+\\
& \sum_{h\in H}\sum_{i\in I_h} v_h z_{hi}+E_\theta\left[f\left(\mathbf{x},\mathbf{m},\mathbf{y},\mathbf{z},\boldsymbol{\theta}\right)\right]
\end{aligned}$$

s.t.

$$\sum_{e\in E} x_{ce}\le 1, \forall c\in C \tag{3.1}$$

$$\sum_{e \in E} x_{re} \leq 1, \forall r \in R \tag{3.2}$$

$$\sum_{e \in E} x_{we} \leq 1, \forall w \in W \tag{3.3}$$

$$\sum_{c \in C} \sum_{e \in E} \hat{f}_{ce} x_{ce} + \sum_{r \in R} \sum_{e \in E} \hat{f}_{re} x_{re} + \sum_{w \in W} \sum_{e \in E} \hat{f}_{we} x_{we} + \sum_{c \in C} \tilde{f}_c m_c + \sum_{r \in R} \tilde{f}_r m_r + \sum_{w \in W} \tilde{f}_w m_w \leq X_{\max} \tag{3.4}$$

$$m_c \leq M_c \sum_{e \in E} x_{ce}, \forall c \in C \tag{3.5}$$

$$m_r \leq M_r \sum_{e \in E} x_{re}, \forall r \in R \tag{3.6}$$

$$m_w \leq M_w \sum_{e \in E} x_{we}, \forall w \in W \tag{3.7}$$

$$\sum_{i \in I_h} z_{hi} \leq 1, \forall h \in H \tag{3.8}$$

$$Z_{\min} \leq \sum_{h \in H} \sum_{i \in I_h} z_{hi} \tag{3.9}$$

$$\sum_{h \in H} \sum_{i \in I_h} z_{hi} \leq Z_{\max} \tag{3.10}$$

$$m_c \geq 0, \forall c \in C \tag{3.11}$$

$$m_r \geq 0, \forall r \in R \tag{3.12}$$

$$m_w \geq 0, \forall w \in W \tag{3.13}$$

$$z_{hi} \in \{0, 1\}, \forall h \in H, i \in I_h \tag{3.14}$$

$$x_{ce} \in \{0, 1\}, \forall c \in C, \forall e \in E \tag{3.15}$$

$$x_{re} \in \{0, 1\}, \forall r \in R, \forall e \in E \tag{3.16}$$

$$x_{we} \in \{0, 1\}, \forall w \in W, \forall e \in E \tag{3.17}$$

$$y_{dck} \in \{0, 1\}, \forall d \in D, \forall c \in C, \forall k \in K_{dc} \tag{3.18}$$

$$y_{crk} \in \{0, 1\}, \forall c \in C, \forall r \in R, \forall k \in K_{cr} \tag{3.19}$$

$$y_{cwk} \in \{0, 1\}, \forall c \in C, \forall w \in W, \forall k \in K_{cw} \tag{3.20}$$

$$y_{rwk} \in \{0, 1\}, \forall r \in R, \forall w \in W, \forall k \in K_{rw} \tag{3.21}$$

Minimization of the total system cost is considered in (TSSP1), which accounts for both the self-built recycling network and external recyclers participating in combinatorial auctions. The total cost consists of two components: (i) fixed expenditures, including construction of the internal network as well as management activities for external recyclers; and (ii) expected operating costs under uncertain scenarios, covering facility processing, waste battery recovery, transportation, auction payments, and penalties for delayed recycling. $E_\theta \left[f\left(\mathbf{x}, \mathbf{m}, \mathbf{y}, \mathbf{z}, \boldsymbol{\theta}\right) \right]$ represents the expected value of second-stage operational costs across all scenarios, where $E_\theta[\cdot]$ denotes the expectation operator, and $f\left(\mathbf{x}, \mathbf{m}, \mathbf{y}, \mathbf{z}, \boldsymbol{\theta}\right)$ represents the second-stage operational cost under scenario θ given first-stage decision variables $\mathbf{x}, \mathbf{m}, \mathbf{y}, \mathbf{z}$.

Constraints (3.1)–(3.3) define binary decision variables corresponding to the location and reinforcement decisions of centers. Constraint (3.4) specifies the total budget limitation for reinforcement investment and capacity reservation. Constraints (3.5)–(3.7) restrict the reserved capacity of different facilities to ensure that capacity does not exceed predefined upper bounds. Constraint (3.8) defines a binary variable for the selection of external recyclers, and it also restricts that at most one bundle solution can be selected in the combinatorial auction. Constraints (3.9) and (3.10) aggregate all selected external recycler bundles and ensure that their values remain within predefined bounds. Constraints (3.11)–(3.13) impose non-negativity conditions on continuous variables. Constraints (3.14)–(3.17) define binary restrictions for external recycler selection variables and facility location variables. Constraints (3.18)–(3.21) ensure that decision variables related to 3PL satisfy binary requirements.
(TSSP2)

$$f(\mathbf{x}, \mathbf{m}, \mathbf{y}, \mathbf{z}, \boldsymbol{\theta}) =$$

$$\min \left\{ \begin{array}{l} \sum\limits_{d \in D} \sum\limits_{c \in C} \sum\limits_{k \in K_{dc}} j_c v^1_{dck\theta} + \sum\limits_{r \in R} \sum\limits_{c \in C} \sum\limits_{k \in K_{cr}} \sum\limits_{l \in \{1,2\}} j_r v^2_{crkl\theta} \\ + \sum\limits_{w \in W} j_w \left(\sum\limits_{c \in C} \sum\limits_{k \in K_{cw}} v^3_{cwk\theta} + \sum\limits_{r \in R} \sum\limits_{k \in K_{rw}} v^3_{rwk\theta} \right) + \\ \sum\limits_{d \in D} \sum\limits_{c \in C} \sum\limits_{k \in K_{dc}} s_{dc} t_{dck} v^1_{dck\theta} + \sum\limits_{c \in C} \sum\limits_{r \in R} \sum\limits_{k \in K_{cr}} \sum\limits_{l \in \{1,2\}} s_{cr} t_{crk} v^2_{crkl\theta} + \sum\limits_{c \in C} \sum\limits_{w \in W} \sum\limits_{k \in K_{cw}} s_{cw} t_{cwk} v^3_{cwk\theta} + \\ \sum\limits_{r \in R} \sum\limits_{w \in W} \sum\limits_{k \in K_{rw}} s_{rw} t_{rwk} v^3_{rwk\theta} + \sum\limits_{d \in D} \vartheta v^{\mathrm{rest}}_{d\theta} + \sum\limits_{c \in C} \sum\limits_{d \in D} \sum\limits_{l \in L} \sum\limits_{k \in K_{dc}} \alpha_l m_l v^1_{dck\theta} + \\ \sum\limits_{h \in H} \sum\limits_{i \in I_h} b_{hi} v^1_{hi\theta} + P_{\mathrm{ct}} T_\theta \end{array} \right\}$$

s.t.

$$\xi_d = \sum_{c \in C} \sum_{k \in K_{dc}} v^1_{dck\theta} + \sum_{h \in H} \sum_{i \in I_h} A_{dhi} v^1_{hi\theta} + v^{\mathrm{rest}}_{d\theta}, \forall d \in D, \forall \theta \in \Theta \tag{3.22}$$

$$\sum_{d \in D} \sum_{k \in K_{dc}} v^1_{dck\theta} \leq \sum_{e \in E} x_{ce} \left[(1 - q_{c\theta}) V_c + q_{c\theta} \lambda_{ce} V_c \right] + m_c, \forall c \in C, \forall \theta \in \Theta \tag{3.23}$$

$$\sum_{c \in C} \sum_{k \in K_{cr}} \sum_{l \in \{1,2\}} v^2_{crkl\theta} \leq \sum_{e \in E} x_{re} \left[(1 - q_{r\theta}) V_r + q_{r\theta} \lambda_{re} V_r \right] + m_r, \forall r \in R, \forall \theta \in \Theta \tag{3.24}$$

$$\sum_{c \in C} \sum_{k \in K_{cw}} v^3_{cwk\theta} + \sum_{r \in R} \sum_{k \in K_{rw}} v^3_{rwk\theta} \leq \sum_{e \in E} x_{we} \left[(1 - q_{w\theta}) V_w + q_{w\theta} \lambda_{we} V_w \right] + m_w, \forall w \in W, \forall \theta \in \Theta \tag{3.25}$$

$$\sum_{d \in D} \sum_{k \in K_{dc}} \alpha_l v^1_{dck\theta} * Num = \sum_{r \in R} \sum_{k \in K_{cr}} v^2_{crkl\theta}, \forall c \in C, l \in \{1, 2\}, \forall \theta \in \Theta \tag{3.26}$$

$$\omega \sum_{d \in D} \sum_{k \in K_{dc}} \alpha_l v^1_{dck\theta} * Num = \sum_{w \in W} \sum_{k \in K_{cw}} v^3_{cwk\theta}, \forall c \in C, \forall \theta \in \Theta, l \in \{3\} \tag{3.27}$$

$$\omega \sum_{c \in C} \sum_{k \in K_{cr}} \sum_{l \in \{1,2\}} v^2_{crkl\theta} \varphi_l = \sum_{w \in W} \sum_{k \in K_{rw}} v^3_{rwk\theta}, \forall r \in R, \forall \theta \in \Theta \tag{3.28}$$

$$v^1_{dck\theta} \leq y_{dck} g_{dck}, \forall d \in D, \forall c \in C, \forall k \in K_{dc}, \forall \theta \in \Theta \tag{3.29}$$

$$\sum_{l \in \{1,2\}} v^2_{crkl\theta} \leq y_{crk} g_{crk}, \forall c \in C, \forall r \in R, \forall k \in K_{cr}, \forall \theta \in \Theta \tag{3.30}$$

$$v_{cwk\theta}^{3} \leq y_{cwk} g_{cwk}, \forall c \in C, \forall w \in W, \forall k \in K_{cw}, \forall \theta \in \Theta \tag{3.31}$$

$$v_{rwk\theta}^{3} \leq y_{rwk} g_{rwk}, \forall r \in R, \forall w \in W, \forall k \in K_{rw}, \forall \theta \in \Theta \tag{3.32}$$

$$v_{hi\theta}^{1} \leq z_{hi} UP_{hi}, \forall h \in H, \forall i \in I_h, \forall \theta \in \Theta \tag{3.33}$$

$$T_\theta = T_{\text{transport},\theta} + T_{\text{process},\theta}, \forall \theta \in \Theta \tag{3.34}$$

$$T_{\text{transport},\theta} = P_{\text{transport}} \left(\begin{array}{l} \sum_{d \in D} \sum_{c \in C} \sum_{k \in K_{dc}} s_{dc} v_{dck\theta}^{1} \hat{\omega} + \sum_{c \in C} \sum_{r \in R} \sum_{k \in K_{cr}} \sum_{l \in \{1,2\}} s_{cr} v_{crkl\theta}^{2} \cdot Num \cdot \omega + \\ \sum_{c \in C} \sum_{w \in W} \sum_{k \in K_{cw}} s_{cw} v_{cwk\theta}^{3} + \sum_{r \in R} \sum_{w \in W} \sum_{k \in K_{rw}} s_{rw} v_{rwk\theta}^{3} \end{array} \right), \forall \theta \in \Theta \tag{3.35}$$

$$T_{\text{process},\theta} = \left(\begin{array}{l} \sum_{d \in D} \sum_{c \in C} \sum_{k \in K_{dc}} P_{\text{process},c} v_{dck\theta}^{1} + \sum_{c \in C} \sum_{r \in R} \sum_{k \in K_{cr}} \sum_{l \in \{1,2\}} P_{\text{process},r} v_{crkl\theta}^{2} + \\ \sum_{c \in C} \sum_{w \in W} \sum_{k \in K_{cw}} P_{\text{process},w} v_{cwk\theta}^{3} + \sum_{r \in R} \sum_{w \in W} \sum_{k \in K_{rw}} P_{\text{process},w} v_{rwk\theta}^{3} \end{array} \right), \forall \theta \in \Theta \tag{3.36}$$

$$T_\theta \leq UB_{\text{carbon}}, \forall \theta \in \Theta \tag{3.37}$$

$$v_{dck\theta}^{1} \geq 0, \forall d \in D, \forall c \in C, \forall k \in K_{dc}, \forall \theta \in \Theta \tag{3.38}$$

$$v_{hi\theta}^{1} \geq 0, \forall h \in H, \forall i \in I_h, \forall \theta \in \Theta \tag{3.39}$$

$$v_{crkl\theta}^{2} \geq 0, \forall c \in C, \forall r \in R, \forall k \in K_{cr}, \forall \theta \in \Theta, l \in \{1,2\} \tag{3.40}$$

$$v_{cwk\theta}^{3} \geq 0, \forall c \in C, \forall w \in W, \forall k \in K_{cw}, \forall \theta \in \Theta \tag{3.41}$$

$$v_{rwk\theta}^{3} \geq 0, \forall r \in R, \forall w \in W, \forall k \in K_{rw}, \forall \theta \in \Theta \tag{3.42}$$

$$v_{d\theta}^{\text{rest}} \geq 0, \forall d \in D, \forall \theta \in \Theta \tag{3.43}$$

In (TSSP2), minimization of total operating cost is considered for both the self-built recycling network and external recyclers. Constraint (3.22) ensures that all end-of-life EVBs generated in collection region (d) are completely allocated. The first term denotes the quantity processed through the self-built recycling network. The second term denotes the quantity handled by external recyclers through the WD mechanism. In this term, ($v_{hi\theta}^{1}$) represents the quantity associated with bid bundle (i) submitted by external recycler (h), while the auxiliary parameter (A_{dhi}) indicates whether collection region (d) is covered by that bundle. Consequently, ($A_{dhi} v_{hi\theta}^{1}$) links the selected bid bundle to the corresponding collection regions and determines whether the quantity associated with that bundle contributes to the demand fulfillment of collection region (d). The last term represents unrecovered end-of-life EVBs. Constraints (3.23)–(3.25) represent the capacity limitations of collection centers, remanufacturing centers, and disposal centers under disruption scenarios. The available processing capacity of a facility depends on both its disruption state and the selected reinforcement level. When no disruption occurs ($q = 0$), the facility operates at its nominal capacity (V). When a disruption occurs ($q = 1$), the available capacity is reduced according to the capacity-retention coefficient (λ_e, e.g., λ_{ce}, λ_{re}, or λ_{we}) associated with the selected reinforcement level. Specifically, ($\lambda_e = 0$) indicates that no effective capacity is retained after disruption, while ($0 < \lambda_e < 1$) represents partial capacity retention under intermediate reinforcement levels. When the highest reinforcement level is adopted, ($\lambda_e = 1$), implying that the facility can maintain its full processing capacity even after a disruption. Therefore, the available capacity under disruption scenarios is determined jointly by the disruption state and the selected reinforcement strategy. Constraints (3.26)–(3.28) are also flow balance constraints that describe flow conservation relationships between nodes in the network, ensuring that inflow and outflow are balanced. Constraints (3.29)–(3.32) represent capacity constraints for 3PL providers, ensuring that transportation tasks do not exceed service capacities. Constraint (3.33) limits the transportation capacity of external recyclers, ensuring that assigned battery flows do not exceed their maximum handling capacity. Constraints (3.34)–(3.37) define the carbon-emission constraints of the recycling network. Carbon-emission accounting focuses on transportation activities and processing operations within the self-built recycling network. Constraint (3.34) defines total system carbon emissions, consisting of transportation emissions and facility processing emissions. Constraint (3.35) specifies the calculation of transportation-related emissions. Constraint (3.36) describes emissions arising from battery or waste processing at collection, remanufacturing, and disposal facilities. An upper limit on total system carbon emissions is enforced by Constraint (3.37). Non-negativity conditions are specified for the relevant decision variables in Constraints (3.38)–(3.43).

In the TSSP model, the evaluation of the expectation term $E_\theta\left[f\left(\mathbf{x},\mathbf{m},\mathbf{y},\mathbf{z},\boldsymbol{\theta}\right)\right]$ constitutes the key difficulty in model solution, where the characterization of scenario probabilities plays a crucial role.

Based on the approach by Snyder and Daskin [40], independence among disruption events of facility nodes is assumed in this study. Accordingly, the probability of each disruption scenario is given as follows:

$$p_\theta=\left[\prod_{\theta\in C_\theta}p_{c\theta}\prod_{\theta\in C\backslash C_\theta}(1-p_{c\theta})\right]\left[\prod_{\theta\in R_\theta}p_{r\theta}\prod_{\theta\in R\backslash R_\theta}(1-p_{r\theta})\right]\left[\prod_{\theta\in W_\theta}p_{w\theta}\prod_{\theta\in W\backslash W_\theta}(1-p_{w\theta})\right]$$

where p_θ represents the joint likelihood of scenario θ; C, R, and W correspond to the sets of recycling, remanufacturing, and disposal centers, respectively; C_θ, R_θ, and W_θ denote the corresponding subsets of facilities that experience disruptions under scenario θ; and $p_{c\theta}$, $p_{r\theta}$, and $p_{w\theta}$ denote the disruption probabilities of different types of facilities.

On this basis, the expectation term in the TSSP model can be expressed as a weighted summation over all scenarios, i.e., $E_\theta\left[f\left(\mathbf{x},\mathbf{m},\mathbf{y},\mathbf{z},\boldsymbol{\theta}\right)\right]=\sum_{\theta\in\Theta}p_\theta\left[f\left(\mathbf{x},\mathbf{m},\mathbf{y},\mathbf{z},\boldsymbol{\theta}\right)\right]$. Accordingly, the original model can be transformed into a deterministic equivalent formulation based on a discrete scenario set (DP).

(DP)

$$\begin{aligned}
&\min\sum_{c\in C}\sum_{e\in E}\left(f_c+\hat{f}_{ce}\right)x_{ce}+\sum_{r\in R}\sum_{e\in E}\left(f_r+\hat{f}_{re}\right)x_{re}+\sum_{w\in W}\sum_{e\in E}\left(f_w+\hat{f}_{we}\right)x_{we}+\\
&\sum_{c\in C}\tilde{f}_c m_c+\sum_{r\in R}\tilde{f}_r m_r+\sum_{w\in W}\tilde{f}_w m_w+\\
&\sum_{d\in D}\sum_{c\in C}\sum_{k\in K_{dc}}f_{dck}y_{dck}+\sum_{c\in C}\sum_{r\in R}\sum_{k\in K_{cr}}f_{crk}y_{crk}+\sum_{c\in C}\sum_{w\in W}\sum_{k\in K_{cw}}f_{cwk}y_{cwk}+\sum_{r\in R}\sum_{w\in W}\sum_{k\in K_{rw}}f_{rwk}y_{rwk}+\\
&\sum_{h\in H}\sum_{i\in I_h}v_h z_{hi}+\\
&\sum_{\theta\in\Theta}p_\theta\left\{\begin{aligned}
&\sum_{d\in D}\sum_{c\in C}\sum_{k\in K_{dc}}j_c v^1_{dck\theta}+\sum_{r\in R}\sum_{c\in C}\sum_{k\in K_{cr}}\sum_{l\in\{1,2\}}j_r v^2_{crkl\theta}\\
&+\sum_{w\in W}j_w\left(\sum_{c\in C}\sum_{k\in K_{cw}}v^3_{cwk\theta}+\sum_{r\in R}\sum_{k\in K_{rw}}v^3_{rwk\theta}\right)+\\
&\sum_{d\in D}\sum_{c\in C}\sum_{k\in K_{dc}}s_{dc}t_{dck}v^1_{dck\theta}+\sum_{c\in C}\sum_{r\in R}\sum_{k\in K_{cr}}\sum_{l\in\{1,2\}}s_{cr}t_{crk}v^2_{crkl\theta}+\sum_{c\in C}\sum_{w\in W}\sum_{k\in K_{cw}}s_{cw}t_{cwk}v^3_{cwk\theta}+\\
&\sum_{r\in R}\sum_{w\in W}\sum_{k\in K_{rw}}s_{rw}t_{rwk}v^3_{rwk\theta}+\sum_{d\in D}\vartheta v^{\text{rest}}_{d\theta}+\sum_{c\in C}\sum_{d\in D}\sum_{l\in L}\sum_{k\in K_{dc}}\alpha_l m_l v^1_{dck\theta}+\\
&\sum_{h\in H}\sum_{i\in I_h}b_{hi}v^1_{hi\theta}+P_{\text{ct}}T_\theta
\end{aligned}\right\}
\end{aligned}$$

Since the (DP) model belongs to the class of mixed-integer linear programming problems, a direct solution can be obtained using commercial solvers such as CPLEX. However, as the number of disruption scenarios grows, model size expands exponentially, and the computational complexity increases significantly, which imposes severe challenges on the solution efficiency of commercial solvers. Therefore, in the next chapter, a hybrid SR-LR is proposed based on scenario reduction and the Lagrangian relaxation method associated with progressive hedging algorithm (PHA) to enhance the computational efficiency of the proposed model.

4. Hybrid scenario reduction and Lagrangian relaxation algorithm

This section develops the SR-LR algorithm framework based on scenario reduction and Lagrangian relaxation. Specifically, the original scenario set is first compressed to generate a reduced representative set. Based on the simplified model, an upper-bound solution to the (DP) model is derived. Furthermore, to compensate for approximation errors introduced by scenario reduction, a lower-bound formulation is established via the Lagrangian relaxation method, forming a collaborative bounding mechanism. Algorithm performance is assessed through the gap between upper and lower bounds. However, since approximation errors are unavoidable in the reduction process, relying solely on the upper-bound solution cannot guarantee solution quality. Therefore, a complementary lower-bound formulation of the (DP) model is further developed using Lagrangian relaxation, and the relative optimality gap is employed to assess effectiveness and solution accuracy. The detailed procedure is outlined below.

4.1. SR method

A scenario reduction approach was introduced by Karuppiah et al. [41], with the core idea of selecting representative high-probability scenarios to substitute for the original high-dimensional scenario set. In this manner, the scenario set size is reduced while preserving key distributional characteristics, and an approximate optimal solution to the original problem is derived.

(SR)

$$\min \sum_{a_1=1}^{2}\sum_{a_2=1}^{2}\cdots\sum_{a_n=1}^{2}\left[\left(1 - x_1^{i_1} x_2^{i_2}\cdots x_n^{i_n}\right)\hat{x}_{a_1,a_2,\cdots a_n}\right]$$

s.t.

$$\sum_{a_2=1}^{2}\sum_{a_3=1}^{2}\cdots\sum_{a_n=1}^{2}\hat{x}_{a_1,a_2,\cdots a_n} = x_1^{a_1}, a_1 = 1\cdots 2 \tag{4.1}$$

$$\sum_{a_1=1}^{2}\sum_{a_3=1}^{2}\cdots\sum_{a_n=1}^{2}\hat{x}_{a_1,a_2,\cdots a_n} = x_2^{a_2}, a_2 = 1\cdots 2 \tag{4.2}$$

$$\vdots$$

$$\sum_{a_1=1}^{2}\sum_{a_2=1}^{2}\cdots\sum_{a_{n-1}=1}^{2}\hat{x}_{a_1,a_2,\cdots a_n} = x_n^{a_n}, a_n = 1\cdots 2 \tag{4.3}$$

$$\sum_{a_1=1}^{2}\sum_{a_2=1}^{2}\cdots\sum_{a_n=1}^{2}\hat{x}_{a_1,a_2,\cdots a_n} = 1 \tag{4.4}$$

$$0 \leq \hat{x}_{a_1,a_2,\cdots a_n} \leq 1, \forall a_1, a_2, \cdots a_n \tag{4.5}$$

where a_n denotes the node set composed of the n-th type of facilities, and $x_n^{a_n}$ denotes the disruption (or normal operation) probability of the corresponding facility under a given scenario. Accordingly, the term $x_1^{a_1} x_2^{a_2} \cdots x_n^{a_n}$ represents the joint probability corresponding to a specific combination of facility states. Furthermore, $\hat{x}_{a_1,a_2,\cdots,a_n}$ is defined as the redistributed joint probability obtained after scenario reduction. In formulating the SR model objective, probability distributions from both the original and reduced scenario sets are taken into account. The goal is to decrease scenario scale while retaining high-probability representative scenarios from the original set, thereby limiting information loss. Constraints (4.1)–(4.3) enforce consistency between the two sets in terms of marginal probability distributions, meaning that the occurrence likelihoods of potential disrupted facilities are preserved. Constraint (4.4) guarantees that the probabilities across all reduced scenarios sum to unity. Constraint (4.5) confines scenario probabilities within the range [0, 1].

By solving the SR formulation, a reduced set of scenarios and the corresponding probability distribution can be obtained. Accordingly, the original deterministic equivalent model (DP) can be transformed into a simplified formulation based on the reduced scenario set, thereby improving subsequent computational efficiency.
(SR-DP)

$$\begin{aligned}
&\min \sum_{c\in C}\sum_{e\in E}\left(f_c + \hat{f}_{ce}\right)x_{ce} + \sum_{r\in R}\sum_{e\in E}\left(f_r + \hat{f}_{re}\right)x_{re} + \sum_{w\in W}\sum_{e\in E}\left(f_w + \hat{f}_{we}\right)x_{we} + \\
&\sum_{c\in C}\tilde{f}_c m_c + \sum_{r\in R}\tilde{f}_r m_r + \sum_{w\in W}\tilde{f}_w m_w + \\
&\sum_{d\in D}\sum_{c\in C}\sum_{k\in K_{dc}} f_{dck}y_{dck} + \sum_{c\in C}\sum_{r\in R}\sum_{k\in K_{cr}} f_{crk}y_{crk} + \sum_{c\in C}\sum_{w\in W}\sum_{k\in K_{cw}} f_{cwk}y_{cwk} + \sum_{r\in R}\sum_{w\in W}\sum_{k\in K_{rw}} f_{rwk}y_{rwk} + \\
&\sum_{h\in H}\sum_{i\in I_h} v_h z_{hi} + \\
&\sum_{\theta\in\hat{\Theta}}\hat{p}_\theta \left\{\begin{aligned}
&\sum_{d\in D}\sum_{c\in C}\sum_{k\in K_{dc}} j_c v^1_{dck\theta} + \sum_{r\in R}\sum_{c\in C}\sum_{k\in K_{cr}}\sum_{l\in\{1,2\}} j_r v^2_{crkl\theta} \\
&+ \sum_{w\in W} j_w\left(\sum_{c\in C}\sum_{k\in K_{cw}} v^3_{cwk\theta} + \sum_{r\in R}\sum_{k\in K_{rw}} v^3_{rwk\theta}\right) + \\
&\sum_{d\in D}\sum_{c\in C}\sum_{k\in K_{dc}} s_{dc}t_{dck}v^1_{dck\theta} + \sum_{c\in C}\sum_{r\in R}\sum_{k\in K_{cr}}\sum_{l\in\{1,2\}} s_{cr}t_{crk}v^2_{crkl\theta} + \sum_{c\in C}\sum_{w\in W}\sum_{k\in K_{cw}} s_{cw}t_{cwk}v^3_{cwk\theta} + \\
&\sum_{r\in R}\sum_{w\in W}\sum_{k\in K_{rw}} s_{rw}t_{rwk}v^3_{rwk\theta} + \sum_{d\in D}\vartheta v^{\text{rest}}_{d\theta} + \sum_{c\in C}\sum_{d\in D}\sum_{l\in L}\sum_{k\in K_{dc}} \alpha_l m_l v^1_{dck\theta} + \\
&\sum_{h\in H}\sum_{i\in I_h} b_{hi}v^1_{hi\theta} + P_{\text{ct}}T_\theta
\end{aligned}\right\}
\end{aligned}$$

s.t. (3.1)–(3.43).

where $\hat{\Theta}$ and $\hat{p}_\theta$ represent the set of disruption scenarios after reduction and the associated scenario probabilities, respectively. Solving the (SR-DP) model yields a feasible solution $(\mathbf{y}', \mathbf{m}', \mathbf{x}', \mathbf{z}')$ for the deterministic equivalent model (DP). By substituting this solution into the original (DP), the first-stage decisions are fixed, converting the problem into the following linear programming formulation (DP-LP):
(DP-LP)

$$\min COST + \sum_{\theta\in\Theta} p_\theta \Delta_\theta$$

s.t. (3.1)-(3.43).

In this model, the fixed cost term $COST$ is determined by the first-stage decision variables. Since $(\mathbf{y}', \mathbf{m}', \mathbf{x}', \mathbf{z}')$ are given, $COST$ becomes a constant term.

Furthermore, the (DP-LP) model admits a decomposition into $|\Theta|$ scenario-specific independent subproblems. For a given scenario θ, each subproblem focuses on minimizing the corresponding operational cost Δ_θ, which is defined as follows:

$$\Delta_\theta = \left\{ \begin{array}{l} \sum\limits_{d\in D}\sum\limits_{c\in C}\sum\limits_{k\in K_{dc}} j_c v^1_{dck\theta} + \sum\limits_{r\in R}\sum\limits_{c\in C}\sum\limits_{k\in K_{cr}}\sum\limits_{l\in\{1,2\}} j_r v^2_{crkl\theta} \\ + \sum\limits_{w\in W} j_w \left(\sum\limits_{c\in C}\sum\limits_{k\in K_{cw}} v^3_{cwk\theta} + \sum\limits_{r\in R}\sum\limits_{k\in K_{rw}} v^3_{rwk\theta} \right) + \\ \sum\limits_{d\in D}\sum\limits_{c\in C}\sum\limits_{k\in K_{dc}} s_{dc} t_{dck} v^1_{dck\theta} + \sum\limits_{c\in C}\sum\limits_{r\in R}\sum\limits_{k\in K_{cr}}\sum\limits_{l\in\{1,2\}} s_{cr} t_{crk} v^2_{crkl\theta} + \sum\limits_{c\in C}\sum\limits_{w\in W}\sum\limits_{k\in K_{cw}} s_{cw} t_{cwk} v^3_{cwk\theta} + \\ \sum\limits_{r\in R}\sum\limits_{w\in W}\sum\limits_{k\in K_{rw}} s_{rw} t_{rwk} v^3_{rwk\theta} + \sum\limits_{d\in D} \vartheta v^{\text{rest}}_{d\theta} + \sum\limits_{c\in C}\sum\limits_{d\in D}\sum\limits_{l\in L}\sum\limits_{k\in K_{dc}} \alpha_l m_l v^1_{dck\theta} + \\ \sum\limits_{h\in H}\sum\limits_{i\in I_h} b_{hi} v^1_{hi\theta} + P_{\text{ct}} T_\theta \end{array} \right\}$$

By solving each scenario subproblem independently, an upper bound of the deterministic equivalent model (DP) can be obtained, which is expressed as $COST + \sum\limits_{\theta\in\Theta} p_\theta \Delta_\theta$.

4.2. Lagrangian relaxation method

A lower-bound solution method for the (DP) model is further developed based on the Lagrangian relaxation approach to assess the quality of the constructed upper bound.

It can be observed that the main difficulty in efficiently solving the (DP) model arises from the first-stage decision variables $(\mathbf{y}_\theta, \mathbf{m}_\theta, \mathbf{x}_\theta, \mathbf{z}_\theta)$ being independent of scenarios, which leads to strong coupling among different scenarios. To enable problem decomposition, auxiliary variables $(\mathbf{y}_\theta, \mathbf{m}_\theta, \mathbf{x}_\theta, \mathbf{z}_\theta)$ are introduced for every scenario $\theta \in \Theta$. To maintain consistency between the decomposed formulation and the original problem, non-anticipativity constraints (4.6) are imposed. Accordingly, the (DP) model is reformulated as follows:

$$\sum_{\theta\in\Theta} p_\theta \left\{ \begin{array}{l} \sum\limits_{c\in C}\sum\limits_{e\in E} \left(f_c + \hat{f}_{ce}\right) x_{ce} + \sum\limits_{r\in R}\sum\limits_{e\in E} \left(f_r + \hat{f}_{re}\right) x_{re} + \sum\limits_{w\in W}\sum\limits_{e\in E} \left(f_w + \hat{f}_{we}\right) x_{we} + \\ \sum\limits_{c\in C} \tilde{f}_c m_c + \sum\limits_{r\in R} \tilde{f}_r m_r + \sum\limits_{w\in W} \tilde{f}_w m_w + \\ \sum\limits_{d\in D}\sum\limits_{c\in C}\sum\limits_{k\in K_{dc}} f_{dck} y_{dck} + \sum\limits_{c\in C}\sum\limits_{r\in R}\sum\limits_{k\in K_{cr}} f_{crk} y_{crk} + \sum\limits_{c\in C}\sum\limits_{w\in W}\sum\limits_{k\in K_{cw}} f_{cwk} y_{cwk} + \sum\limits_{r\in R}\sum\limits_{w\in W}\sum\limits_{k\in K_{rw}} f_{rwk} y_{rwk} + \\ \sum\limits_{h\in H}\sum\limits_{i\in I_h} v_h z_{hi} + \\ \sum\limits_{d\in D}\sum\limits_{c\in C}\sum\limits_{k\in K_{dc}} j_c v^1_{dck\theta} + \sum\limits_{r\in R}\sum\limits_{c\in C}\sum\limits_{k\in K_{cr}}\sum\limits_{l\in\{1,2\}} j_r v^2_{crkl\theta} \\ + \sum\limits_{w\in W} j_w \left(\sum\limits_{c\in C}\sum\limits_{k\in K_{cw}} v^3_{cwk\theta} + \sum\limits_{r\in R}\sum\limits_{k\in K_{rw}} v^3_{rwk\theta} \right) + \\ \sum\limits_{d\in D}\sum\limits_{c\in C}\sum\limits_{k\in K_{dc}} s_{dc} t_{dck} v^1_{dck\theta} + \sum\limits_{c\in C}\sum\limits_{r\in R}\sum\limits_{k\in K_{cr}}\sum\limits_{l\in\{1,2\}} s_{cr} t_{crk} v^2_{crkl\theta} + \sum\limits_{c\in C}\sum\limits_{w\in W}\sum\limits_{k\in K_{cw}} s_{cw} t_{cwk} v^3_{cwk\theta} + \\ \sum\limits_{r\in R}\sum\limits_{w\in W}\sum\limits_{k\in K_{rw}} s_{rw} t_{rwk} v^3_{rwk\theta} + \sum\limits_{d\in D} \vartheta v^{\text{rest}}_{d\theta} + \sum\limits_{c\in C}\sum\limits_{d\in D}\sum\limits_{l\in L}\sum\limits_{k\in K_{dc}} \alpha_l m_l v^1_{dck\theta} + \\ \sum\limits_{h\in H}\sum\limits_{i\in I_h} b_{hi} v^1_{hi\theta} + P_{\text{ct}} T_\theta \end{array} \right\}$$

s.t. (3.1)–(3.43).

$$(\mathbf{y}_\theta, \mathbf{m}_\theta, \mathbf{x}_\theta, \mathbf{z}_\theta) = (\mathbf{y}_{\theta'}, \mathbf{m}_{\theta'}, \mathbf{x}_{\theta'}, \mathbf{z}_{\theta'}), \theta \in \Theta, \theta' \in \Theta, \theta \neq \theta' \tag{4.6}$$

The constraint (4.6) enforces consistency across different scenarios; however, it also significantly increases the difficulty of solving the model. Inspired by the PHA, a set of consensus variables $(\bar{\mathbf{y}}, \bar{\mathbf{m}}, \bar{\mathbf{x}}, \bar{\mathbf{z}})$ is introduced, and the non-anticipativity constraints can be reformulated as deviation constraints between scenario-dependent variables and the consensus variables, i.e.,

$$(\bar{\mathbf{y}}, \bar{\mathbf{m}}, \bar{\mathbf{x}}, \bar{\mathbf{z}}) = (\mathbf{y}_\theta, \mathbf{m}_\theta, \mathbf{x}_\theta, \mathbf{z}_\theta), \theta \in \Theta \tag{4.7}$$

On this basis, a Lagrangian multiplier vector $\boldsymbol{\lambda}$ is introduced to relax the consistency constraints, and the Lagrangian relaxation model (DP-LR) is obtained.

Given $\boldsymbol{\lambda}$ as the Lagrangian multiplier vector, constraint (4.7) is relaxed, and the Lagrangian relaxation formulation (DP-LR) is expressed as follows:
(DP-LR)

$$\sum_{\theta \in \Theta} p_\theta \left\{ \begin{array}{l} \sum\limits_{c \in C} \sum\limits_{e \in E} \left(f_c + \hat{f}_{ce}\right) x_{ce} + \sum\limits_{r \in R} \sum\limits_{e \in E} \left(f_r + \hat{f}_{re}\right) x_{re} + \sum\limits_{w \in W} \sum\limits_{e \in E} \left(f_w + \hat{f}_{we}\right) x_{we} + \\ \sum\limits_{c \in C} \tilde{f}_c m_c + \sum\limits_{r \in R} \tilde{f}_r m_r + \sum\limits_{w \in W} \tilde{f}_w m_w + \\ \sum\limits_{d \in D} \sum\limits_{c \in C} \sum\limits_{k \in K_{dc}} f_{dck} y_{dck} + \sum\limits_{c \in C} \sum\limits_{r \in R} \sum\limits_{k \in K_{cr}} f_{crk} y_{crk} + \sum\limits_{c \in C} \sum\limits_{w \in W} \sum\limits_{k \in K_{cw}} f_{cwk} y_{cwk} + \sum\limits_{r \in R} \sum\limits_{w \in W} \sum\limits_{k \in K_{rw}} f_{rwk} y_{rwk} + \\ \sum\limits_{h \in H} \sum\limits_{i \in I_h} v_h z_{hi} + \\ \sum\limits_{d \in D} \sum\limits_{c \in C} \sum\limits_{k \in K_{dc}} j_c v^1_{dck\theta} + \sum\limits_{r \in R} \sum\limits_{c \in C} \sum\limits_{k \in K_{cr}} \sum\limits_{l \in \{1,2\}} j_r v^2_{crkl\theta} \\ + \sum\limits_{w \in W} j_w \left(\sum\limits_{c \in C} \sum\limits_{k \in K_{cw}} v^3_{cwk\theta} + \sum\limits_{r \in R} \sum\limits_{k \in K_{rw}} v^3_{rwk\theta} \right) + \\ \sum\limits_{d \in D} \sum\limits_{c \in C} \sum\limits_{k \in K_{dc}} s_{dc} t_{dck} v^1_{dck\theta} + \sum\limits_{c \in C} \sum\limits_{r \in R} \sum\limits_{k \in K_{cr}} \sum\limits_{l \in \{1,2\}} s_{cr} t_{crk} v^2_{crkl\theta} + \sum\limits_{c \in C} \sum\limits_{w \in W} \sum\limits_{k \in K_{cw}} s_{cw} t_{cwk} v^3_{cwk\theta} + \\ \sum\limits_{r \in R} \sum\limits_{w \in W} \sum\limits_{k \in K_{rw}} s_{rw} t_{rwk} v^3_{rwk\theta} + \sum\limits_{d \in D} \vartheta v^{\text{rest}}_{d\theta} + \sum\limits_{c \in C} \sum\limits_{d \in D} \sum\limits_{l \in L} \sum\limits_{k \in K_{dc}} \alpha_l m_l v^1_{dck\theta} + \\ \sum\limits_{h \in H} \sum\limits_{i \in I_h} b_{hi} v^1_{hi\theta} + P_{\text{ct}} T_\theta + \boldsymbol{\lambda}^{\text{T}} \left[(\mathbf{y}_\theta, \mathbf{m}_\theta, \mathbf{x}_\theta, \mathbf{z}_\theta) - (\bar{\mathbf{y}}, \bar{\mathbf{m}}, \bar{\mathbf{x}}, \bar{\mathbf{z}}) \right] \end{array} \right\}$$

s.t. (3.1)-(3.43).

Since the coupling constraints are relaxed, the problem can be decomposed into $|\Theta|$ mutually independent subproblems, thereby significantly improving computational efficiency. Furthermore, an effective lower bound for the (DP) model is obtained by solving the corresponding Lagrangian dual model (DP-LD).
(DP-LD)

$$LD(\boldsymbol{\lambda}) = \max_{\boldsymbol{\lambda}} LR(\boldsymbol{\lambda})$$

Given that the Lagrangian dual problem is non-smooth and concave, a subgradient method is applied to solve the problem. The detailed procedure is outlined below.
Step 1. Initialization.

Set iteration counter $k = 1$, initialize Lagrangian multipliers $\boldsymbol{\lambda}^1$, and set the consensus variables as $(\bar{\mathbf{y}}, \bar{\mathbf{m}}, \bar{\mathbf{x}}, \bar{\mathbf{z}})^0 = \mathbf{0}$.
Step 2. Subproblem solution and lower bound update.

Given λ^k, each scenario $\theta \in \Theta$ is solved independently for the corresponding Lagrangian subproblem, yielding the optimal solution

$$(\mathbf{y}_\theta^*, \mathbf{m}_\theta^*, \mathbf{x}_\theta^*, \mathbf{z}_\theta^*),$$

and the current value of the Lagrangian function $LR(\lambda^k)$ is computed. The best historical lower bound is updated as

$$\Phi^* = \max\left\{\Phi^*, LR\left(\lambda^k\right)\right\}.$$

Step 3. Subgradient computation and multiplier update.

For each scenario θ, the subgradient of the consistency constraints is defined as

$$\mathbf{g}_\theta^k = \left(\mathbf{y}_\theta^* - \bar{\mathbf{y}}^{k-1}, \mathbf{m}_\theta^* - \bar{\mathbf{m}}^{k-1}, \mathbf{x}_\theta^* - \bar{\mathbf{x}}^{k-1}, \mathbf{z}_\theta^* - \bar{\mathbf{z}}^{k-1}\right).$$

The Lagrangian multipliers are updated as

$$\lambda_\theta^{k+1} = \lambda_\theta^k + s^k \mathbf{g}_\theta^k.$$

Following Yin et al. [42], the step size is defined as

$$s^k = \alpha^k \frac{\beta^k - LR\left(\lambda^k\right)}{\left\|\sum_{\theta\in\Theta} \mathbf{g}_\theta^k\right\|^2},$$

where

$$\alpha^k = \varepsilon'(k), \beta^k = [1 + \varepsilon(k)]\,\Phi^*.$$

Step 4. Consensus variable update.

$$(\bar{\mathbf{y}}, \bar{\mathbf{m}}, \bar{\mathbf{x}}, \bar{\mathbf{z}})^k = \frac{1}{|\Theta|} \sum_{\theta\in\Theta} (\mathbf{y}_\theta^*, \mathbf{m}_\theta^*, \mathbf{x}_\theta^*, \mathbf{z}_\theta^*)^k.$$

Step 5. Convergence check.

If the following condition is satisfied:

$$\frac{1}{|\Theta|} \sum_{\theta\in\Theta} \left\|\mathbf{g}_\theta^k\right\| \le \varepsilon,$$

then stop; otherwise, set $k = k + 1$ and return to Step 2.

The proposed Lagrangian relaxation algorithm provides a valid lower bound for the (DP) model. Solution quality is assessed by the difference between upper and lower bounds. A smaller gap implies that the upper-bound solution derived from scenario reduction is closer to optimality, thereby demonstrating the effectiveness and stability of the proposed algorithm.

5. Real-world case and experiments

Numerical experiments are carried out using a real-world case from Jiangxi Province, China, to validate the proposed EVB recycling network model and the SR-LR hybrid algorithm. The model's practical applicability is examined under realistic operating conditions. Furthermore, multiple experimental settings are designed to assess algorithm performance, robustness, and computational efficiency, while also exploring how key parameters and policy variables affect network decisions. Subsection 5.1 introduces the case background, network structure, and data sources; Subsection 5.2 evaluates and compares algorithm performance; and Subsection 5.3 conducts sensitivity analysis.

5.1. Real-world case and data sources

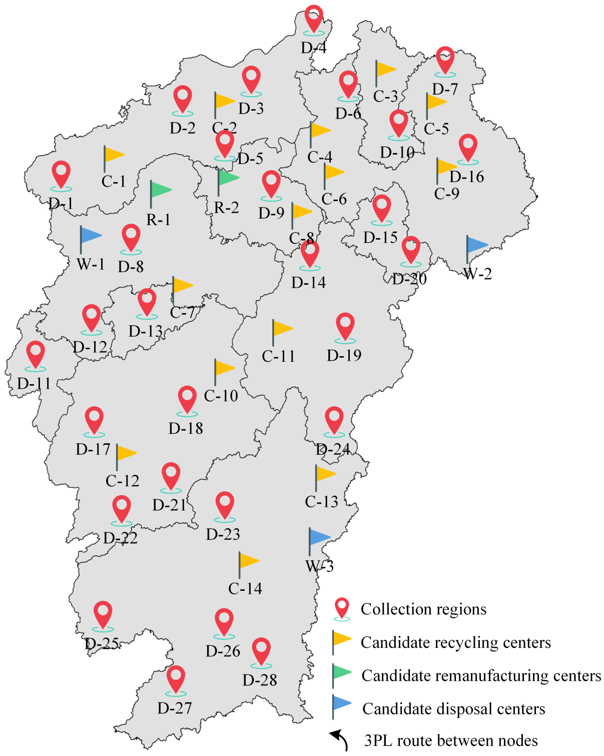

Figure 2. Spatial layout for the EVB recycling network.

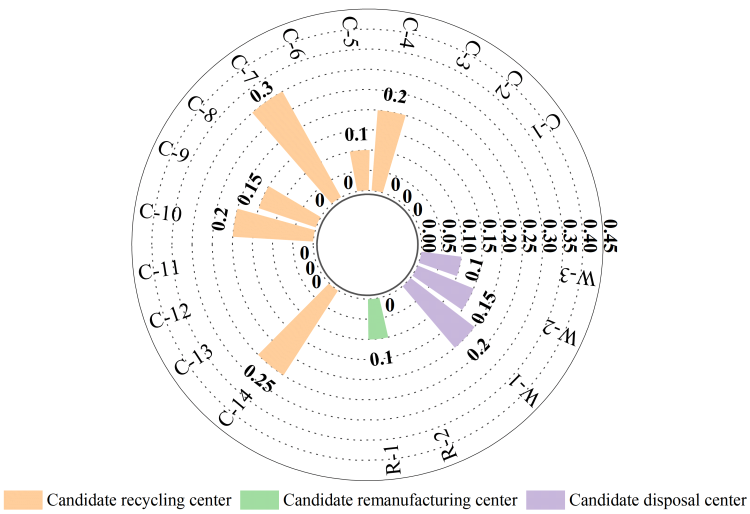

Figure 3. Disruption probability distribution of facilities.

Table 3. Fixed parameters for the EVB recycling network model.

Parameters	Value	Unit
Weight per battery pack	365	kg
Total battery cells per battery pack	96	cell
Weight per battery cell	3.5	kg
Proportion of batteries at different levels ($L1/L2/L3$)	0.15/0.65/0.2	
Unit recycling cost of batteries within the internal network ($L1/L2/L3$)	850/220/100	USD
Proportion of end-of-life battery cells contained in each battery level ($L1/L2$)	0.15/0.2	
Unit penalty cost for unrecovered batteries	5660	USD
Upper bound for facility reinforcement and capacity reservation	500,000	USD
Number of 3PL providers between each pair of locations	2	
Number of external recyclers ($Z_{\min}/Z_{\max}$)	0/6	
Number of bundles handled by each external recycler	5	
Retained processing capacity ($\lambda_{ce}, \lambda_{re}, \lambda_{we}$) under different reinforcement levels ($E0/E1/E2$)	0/(0,1)/1	

*Note: Data sources: The parameter values are adopted from Wang et al. [11], Wang et al. [12], and Li et al. [38]. $L1$–$L3$ denote battery recovery levels, where $L1$ and $L2$ are reusable, while $L3$ is non-reusable. $E0$–$E2$ denote facility reinforcement levels, corresponding to no, basic, and advanced reinforcement, respectively.

This study considers Jiangling Motors Corporation, Ltd. and Dongfeng Motor Corporation Ltd. in Jiangxi Province, China, as the real-world case. Based on publicly available industry reports and related literature (Wang et al., [12]), the network structure constructed in this study is illustrated in Figure 2. Specifically, the system includes 28 collection regions, 14 candidate collection centers, 2 candidate remanufacturing centers, and 3 candidate disposal centers. These facilities together form a multi-stage closed-loop recycling network, where end-of-life power batteries are transferred and processed through different pathways, including recycling, remanufacturing, and disposal, depending on their condition and residual value.

In addition, to capture operational uncertainty and potential disruption risks in real-world environments, different disruption probabilities are assigned to different types of facilities, and the corresponding distribution is presented in Figure 3. Table 3 provides the fixed parameters of the recycling network model, including battery physical characteristics, cost parameters, system structure settings, and technical classification assumptions. Table 4 summarizes the parameter ranges used in the numerical experiments, covering key factors such as demand uncertainty, facility construction costs, operational costs, 3PL transportation costs, capacity constraints, and external recycler-related parameters. Furthermore, Table 5 presents the carbon emission-related parameters incorporated into the model to characterize environmental impacts, including carbon tax levels, transportation emission factors, emission coefficients of processing activities at different facilities, and the upper bound of total system carbon emissions.

Table 4. Parameter ranges for numerical experiments.

Parameters	Value		Unit
	Min	Max	
Recycling demand in each collection region	50	200	pack
Unit construction cost of facilities			
Candidate collection centers	200,000	300,000	USD/center
Candidate remanufacturing centers	600,000	800,000	USD/center
Candidate disposal centers	300,000	600,000	USD/center
Unit reinforcement cost of facilities			
Candidate collection centers ($E0/E1/E2$)	0/500/1000	0/1000/1500	USD/center
Candidate remanufacturing centers ($E0/E1/E2$)	0/300/1000	0/600/1300	USD/center
Candidate disposal centers ($E0/E1/E2$)	0/300/1000	0/700/1300	USD/center
Unit reservation cost of facilities			
Candidate collection centers	10	130	USD/(pack·center)
Candidate remanufacturing centers	20	50	USD/(cell·center)
Candidate disposal centers	20	90	USD/(cell·center)
Unit processing cost of facilities			
Candidate collection centers	500	800	USD/(pack·center)
Candidate remanufacturing centers	10	30	USD/(cell·center)
Candidate disposal centers	0.01	0.03	USD/(cell·center)
Upper bound of processing cost			
Candidate collection centers	700	1900	USD/center
Candidate remanufacturing centers	180,000	250,000	USD/center
Candidate disposal centers	150,000	210,000	USD/center
Upper bound of reservation cost			
Candidate collection centers	400	2000	USD/center
Candidate remanufacturing centers	1000	1700	USD/center
Candidate disposal centers	200	700	USD/center
3PL setup cost			
Collection regions → Candidate collection centers	500	1500	USD/3PL
Candidate collection centers → Candidate remanufacturing centers	500	1500	USD/3PL

Continued on next page

Parameters	Value		Unit
	Min	Max	
Candidate collection centers → Candidate disposal centers	500	1500	USD/3PL
Candidate remanufacturing centers → Candidate disposal centers	500	1500	USD/3PL
3PL unit transportation cost			
Collection regions → Candidate collection centers	7	8.5	USD/(pack·km)
Candidate collection centers → Candidate remanufacturing centers	0.06	0.095	USD/(cell·km)
Candidate collection centers → Candidate disposal centers	0.01	0.015	USD/(kg·km)
Candidate remanufacturing centers → Candidate disposal centers	0.01	0.015	USD/(kg·km)
Upper bound of 3PL transportation capacity			
Collection regions → Candidate collection centers	1200	3500	pack/3PL
Candidate collection centers → Candidate remanufacturing centers	20,000	60,000	cell/3PL
Candidate collection centers → Candidate disposal centers	10,000	40,000	kg/3PL
Candidate remanufacturing centers → Candidate disposal centers	20,000	110,000	kg/3PL
External recycler parameters			
External recycler management cost	8000	10000	USD
Upper bound on bundle size for external recyclers	50	300	pack
Unit bidding price per battery offered by external recyclers	500	1500	USD/pack

*Note: Data Sources: The parameter values are set with reference to Yin et al. [7], Wang et al. [11], Yin et al. [43], and Wang et al. [44]. $E0$, $E1$, and $E2$ denote facility reinforcement levels, corresponding to no reinforcement, basic reinforcement, and advanced reinforcement, respectively. The auxiliary matrix coefficients A_{dhi}, which indicate the assignment of bundles from external recyclers to collection regions D, are provided in Appendix A.

Table 5. Carbon emission-related parameter values.

Parameters	**Value**	**Unit**
Unit carbon tax rate	0.044	USD/kg
Unit carbon emissions from transportation	2.49×10^{-6}	kg CO_2/(kg·km)
Unit carbon emissions from processing at collection centers	233.28	kg CO_2/pack
Unit carbon emissions from processing at remanufacturing centers	31.03	kg CO_2/cell
Unit carbon emissions from processing at disposal centers	0.1	kg CO_2/kg
Upper bound of total carbon emissions	5,000,000	kg

*Note: Data sources: The parameter values are set with reference to Wang et al. [12].

Table 6. Model size under different numbers of disruption scenarios.

Number of scenarios	First-stage status	BV	CV	TV	Constraints
Full model (1024 scenarios)	Optimized	1023	1,109,011	1,110,034	2,162,752
Reduced model (4 scenarios)	Optimized	966	4351	5374	9532
Evaluation model (1024 scenarios)	Fixed	0	1,108,992	1,108,992	2,161,664

*Note: BV, CV, and TV denote binary variables, continuous variables, and total variables, respectively. In the evaluation model, the first-stage decisions obtained from the reduced model are fixed and evaluated under the original 1024-scenario set.

Table 7. Representative scenarios retained after scenario reduction.

Scenario	Disrupted facilities	Probability
S1	None	0.70
S2	C4, C7, C9, C10, C14, W1	0.15
S3	C5, C7, C14, R1, W2, W3	0.10
S4	C4, C7, C10, W1, W2	0.05

Table 8. Convergence of Lagrangian relaxation lower bounds and exponential fitting results.

ϑ	UB_{carbon}	**Exponential fitting curve**	**Lagrangian relaxation iteration plot**
5660	2500000	$y = 10356261.29 - 29220.98e^{-0.005x}$	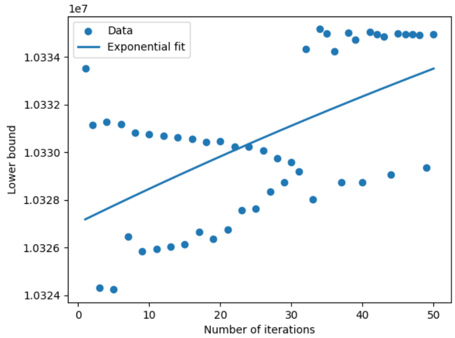
5660	5000000	$y = 9973377.27 - 26379.63e^{-0.005x}$	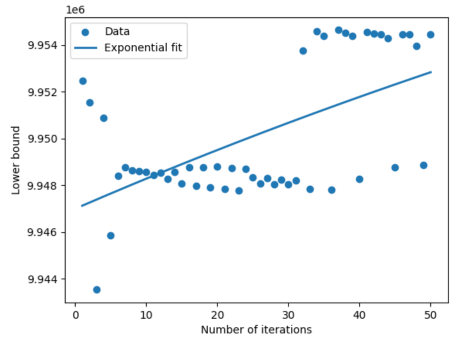
7000	2500000	$y = 11455987.57 - 23464.93e^{-0.005x}$	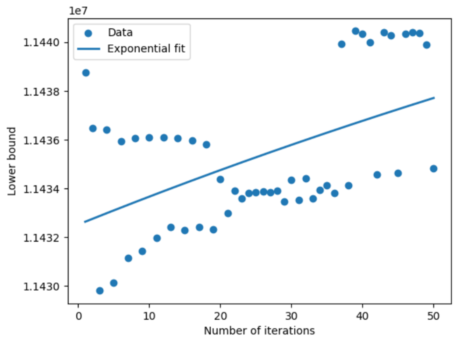
7000	5000000	$y = 10282927.78 - 21311.87e^{-0.005x}$	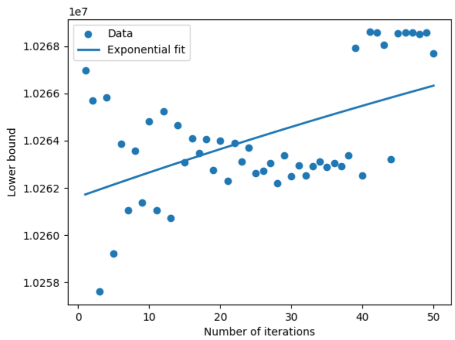

Table 9. Step-size evolution for Lagrangian relaxation under different parameter settings.

Scenario group	Step-size coefficients (α^k, β^k)	Step size per iteration
$\vartheta = 5660$, $UB_{\text{carbon}} = 2500000$	$\alpha^k = 4.5-(0.0882 \cdot k)$, $\beta^k = 2.1-(0.021 \cdot k)$	701.29, 1122.60, 1001.26, 1289.92, 1043.09, 2157.02, 2140.15, 1616.28, 1558.92, 1443.57, 1416.33, 1308.43, 1280.58, 1179.92, 1151.65, 1316.39, 1289.84, 952.06, 914.32, 1037.92, 1009.17, 933.33, 851.28, 1048.52, 1004.58, 976.51, 1014.26, 1133.88, 1040.48, 1818.18, 0.05, 0.46, 0.04, 0.09, 0.08, 0.29, 0.03, 0.05, 0.19, 0.02, 0.03, 0.03, 0.09, 0.01, 0.01, 0.01, 0.01, 0.02, 0.00, 0.00
$\vartheta = 5660$, $UB_{\text{carbon}} = 5000000$	$\alpha^k = 4-(0.0784 \cdot k)$, $\beta^k = 2.1-(0.021 \cdot k)$	489.79, 1487.18, 1223.50, 2716.86, 1618.79, 2003.02, 1764.66, 1750.66, 1612.30, 1594.11, 1464.85, 1444.88, 1324.46, 1081.30, 1191.34, 1168.35, 1065.06, 1041.10, 945.84, 921.19, 833.69, 1082.61, 963.99, 703.37, 833.52, 810.74, 713.90, 689.45, 602.95, 577.97, 0.05, 0.40, 0.04, 0.07, 0.28, 0.03, 0.05, 0.04, 0.16, 0.01, 0.03, 0.02, 0.02, 0.06, 0.00, 0.01, 0.01, 0.02, 0.00, 0.00
$\vartheta = 7000$, $UB_{\text{carbon}} = 2500000$	$\alpha^k = 4-(0.0784 \cdot k)$, $\beta^k = 2.1-(0.021 \cdot k)$	690.05, 1107.90, 982.31, 1235.68, 1179.46, 1093.28, 1040.47, 1143.47, 1085.01, 1461.77, 1353.83, 1660.22, 1522.85, 1497.14, 1369.57, 1797.41, 1619.22, 1598.63, 1102.47, 1176.19, 991.89, 1184.23, 1105.90, 808.52, 724.71, 695.96, 620.19, 754.04, 542.99, 478.59, 451.49, 394.40, 469.40, 330.02, 374.92, 0.03, 0.25, 0.02, 0.04, 0.04, 0.13, 0.01, 0.02, 0.07, 0.01, 0.01, 0.01, 0.00, 0.01, 0.00
$\vartheta = 7000$, $UB_{\text{carbon}} = 5000000$	$\alpha^k = 4-(0.08 \cdot k)$, $\beta^k = 2.1-(0.022 \cdot k)$	416.84, 972.41, 874.25, 1456.52, 1137.78, 1378.44, 1245.72, 1248.00, 993.60, 1563.31, 1030.04, 1478.39, 1148.43, 1849.77, 1252.68, 1614.11, 1164.22, 1304.48, 1277.00, 954.70, 742.57, 1478.11, 1383.68, 886.62, 671.26, 754.31, 548.57, 660.64, 428.55, 534.27, 467.64, 613.28, 561.53, 476.86, 303.50, 419.68, 589.87, 0.02, 0.16, 0.01, 0.02, 0.02, 0.06, 0.00, 0.01, 0.00, 0.00, 0.00, 0.00, 0.00

5.2. *Algorithm analysis*

The effectiveness and computational performance of the proposed SR-LR algorithm are evaluated through analyses from two perspectives, namely upper-bound generation and lower-bound estimation. The SR method is employed to construct a simplified problem and rapidly obtain a feasible solution, thereby providing an upper bound of the original problem. To further illustrate the computational complexity of the proposed two-stage stochastic programming model and the effectiveness of the scenario reduction procedure, the model sizes before and after scenario reduction are summarized in Table 6. The original problem contains 1024 disruption scenarios, resulting in a large number of scenario-dependent decision variables and constraints. After applying the SR method, the scenario set is reduced to four representative scenarios, which significantly decreases the model size and computational burden. The retained representative scenarios and their corresponding probabilities are reported in Table 7. The first-stage decisions obtained from the reduced problem are subsequently fixed and evaluated under the original 1024-scenario environment to generate a feasible solution for the full-scale stochastic program. As shown in Table 7, the reduced scenario set preserves the representative disruption patterns while substantially reducing the computational burden of the original stochastic program.

Meanwhile, the LR method is used to estimate the lower bound of the problem, and the solution range is progressively tightened through an iterative process. The maximum number of LR iterations is set to 50, and the convergence behavior of the lower bound throughout the iterative process is illustrated in Table 8 through embedded iteration plots. Under different parameter settings, four representative scenarios are selected for analysis (unit penalty cost of unrecovered batteries set to 5660 and 7000 USD, and maximum carbon emission caps set to 2,500,000 and 5,000,000, respectively). The iteration process of the Lagrangian relaxation algorithm is analyzed under these scenarios. The variation of the lower bound with respect to iteration number and the corresponding fitted curves are presented in Table 8. The maximum number of LR iterations is set to 50. Different step-size coefficient functions are adopted under different parameter settings to maintain the stability of multiplier updates, and the step size is adjusted dynamically throughout the iterative process. Table 9 summarizes the adopted step-size coefficient functions together with the corresponding step-size values generated during the 50 iterations. The convergence results shown in Table 8 are obtained under these step-size updating rules. It can be observed that the lower bound obtained by the Lagrangian relaxation algorithm does not exhibit monotonic improvement in the early stage of iteration, but instead shows a fluctuation pattern characterized by an initial decrease followed by a recovery. This behavior is mainly attributed to the fact that Lagrangian multipliers have not yet reached suitable values in the early iterations, leading to a temporary exploration phase in the solution space. As iterations proceed, the lower bound gradually increases with oscillations and exhibits an approximately exponential growth trend, as indicated by the fitted curves. Although certain step-like variations are observed in the middle and later stages of iteration, the lower bound overall surpasses the initial level and gradually stabilizes. This indicates that continuous updating of multipliers enables the algorithm to effectively escape local fluctuations and finally provides a reliable estimation of the original problem's lower bound.

To assess the computational efficiency and stability of the proposed SR-LR algorithm under large-scale scenarios, a comparative study is carried out between the SR-LR algorithm and the CPLEX solver. As the scenario size increases, the problem scale grows exponentially, thereby significantly increasing the difficulty of model solving. In each scenario, only facilities affected by disruptions are perturbed, while all other facilities remain in normal operation. All experiments are performed on a Windows 10 system equipped with a 2.60 GHz CPU and 16 GB of RAM. The full model is solved by CPLEX 12.10.0, with the MIP optimality gap set to 0.01%. On this basis, the final obtained lower bounds (i.e., the maximum lower bound values achieved during the Lagrangian relaxation iterations) under each scenario and their comparison with CPLEX results are reported in Table 10. It can be observed that, under small-scale or relatively relaxed constraint settings, the SR-LR algorithm can quickly obtain solutions identical or very close to those of CPLEX, while significantly reducing computational time. As problem scale and complexity increase, the computational burden of CPLEX increases substantially, and feasible solutions cannot even be obtained within an acceptable time horizon in certain scenarios. In contrast, the SR-LR algorithm can still provide stable and effective lower-bound estimates within a relatively short time. Overall, the proposed SR-LR algorithm can significantly reduce computational complexity and solution time while maintaining solution quality, demonstrating strong computational efficiency and robustness. The algorithm is particularly suitable for large-scale scenarios and complex constraint settings in EVB recycling network design problems.

Table 10. Performance comparison between CPLEX and SR-LR.

ϑ	UB_{carbon}	CPLEX		SR-LR			
		Value	Time	Upper bound	Lower bound	Gap (%)	Time
4000	1000000	7555902	12min53s	7555902	7555902	0	3 s
	2500000	7555902	13min48s	7555902	7555902	0	3 s
	5000000	7555902	15min45s	7555902	7555902	0	3s
5660	1000000	10500742	2h21min5s	10500742	10500742	0	3 s
	2500000	NS	NS	10335971.2	10335157.05	0.0079	8 s
	5000000	NS	NS	9954911.36	9954637.8	0.0027	15 s
7000	1000000	NS	NS	12877901	12877901	0	4 s
	2500000	NS	NS	11441225.9	11440459.27	0.0067	27 s
	5000000	NS	NS	10269444	10268599.76	0.0082	37 s

*Note: NS indicates that CPLEX failed to obtain a valid solution for the corresponding instance because of excessive computational requirements, including memory and model-size limitations.

5.3. *Sensitivity analysis*

To further analyze the impact of key parameter variations on EVB recycling network design and system performance, sensitivity analysis is conducted based on the benchmark scenario. The analysis focuses on the effects of core parameters, including the unit penalty cost of unrecovered batteries and the maximum carbon emission cap, on network configuration, recycling scale, and total system cost.

5.3.1. Impact of carbon emission constraint

To investigate the impact of carbon emission constraints on EVB recycling network design, sensitivity analysis is performed on the maximum carbon emission cap $U_{B_{carbon}}$, under the condition that the unit penalty cost of unrecovered batteries is fixed at 7000 USD. The value of $U_{B_{carbon}}$ varies from 1,000,000 to 5,000,000.

Figure 4 illustrates the composition of system costs, recycling performance, and carbon emission variations under different carbon emission constraint levels, while Figure 5 further presents the evolution of the recycling network structure and transportation routes under the corresponding scenarios.

First, Figure 4(a–c) shows that with the gradual relaxation of the carbon emission cap, the internal network operational cost increases significantly, while the network construction cost exhibits only a slight increase. This indicates that under strict carbon constraints, system operations are compressed to control carbon emissions, whereas relaxed constraints lead to higher utilization of internal facilities and increased operational costs.

Figure 4(b) shows that the penalty cost of unrecovered batteries decreases significantly with the increase in the carbon emission cap (from 12.418 million USD to 1.543 million USD), while the internal recycling cost continues to increase. This phenomenon indicates that under looser carbon constraints, the system increases recycling activities to reduce high penalty costs, thereby achieving overall cost optimization.

Figure 4(d–e) shows that total system cost decreases monotonically as the carbon emission cap increases, while the number of recycled batteries increases significantly, and the number of unrecovered batteries decreases markedly. This result suggests a potential conflict between carbon-emission control and recycling targets. Under excessively strict carbon caps, the system tends to reduce recycling and processing activities in order to satisfy environmental requirements, which may lead to a larger number of unrecovered batteries and higher penalty costs. Therefore, carbon-emission policies should be designed carefully to balance environmental objectives and recycling-performance targets.

In terms of environmental impact, Figure 4(f) shows that both transportation-related and processing-related carbon emissions increase as the carbon emission cap is relaxed, with processing-related emissions dominating total emissions. This indicates that facility processing activities are the primary source of carbon emissions in the recycling network compared with transportation activities.

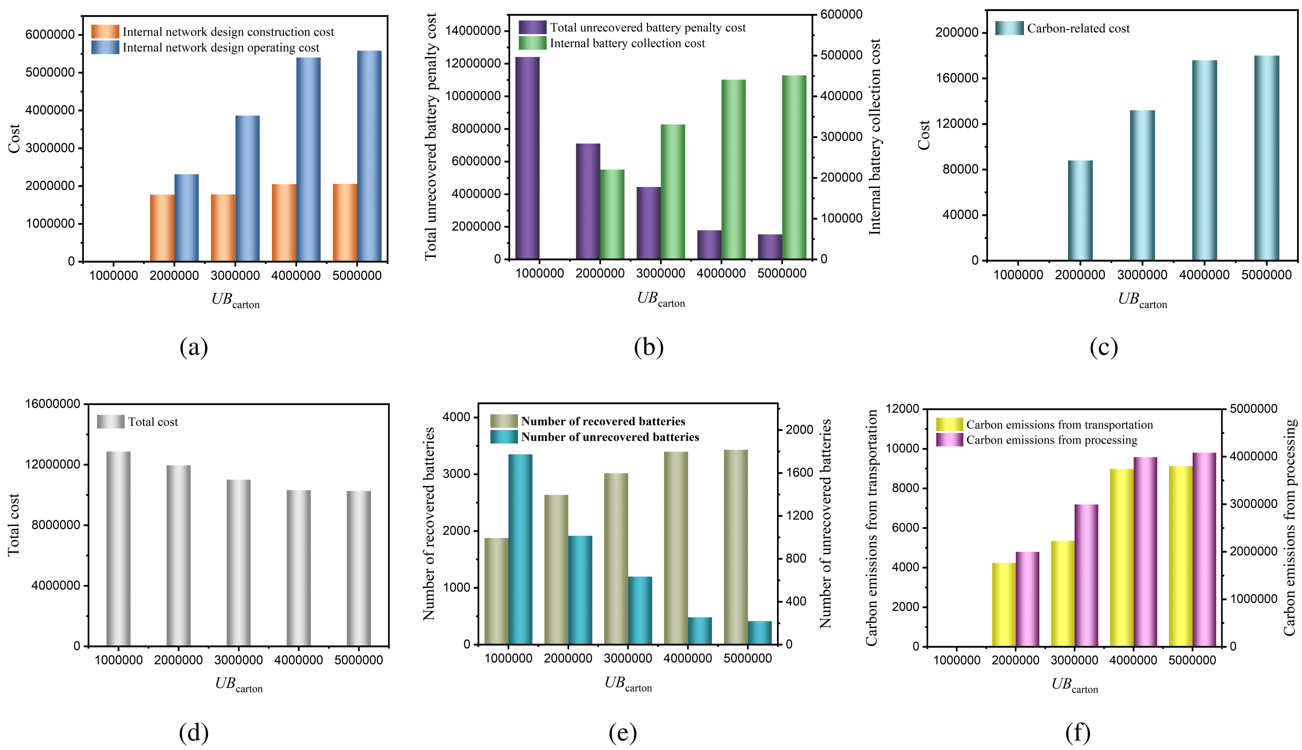

Figure 4. Impact of carbon emission constraints on network performance.

From a network structure perspective, Figure 5 clearly reflects the evolutionary characteristics of the network topology under different carbon constraints. With a relatively low carbon emission cap (e.g., $U_{B_{carbon}} = 1,000,000$), internal recycling and processing facilities remain inactive, and the system exhibits a configuration without internal network deployment. This indicates that under strict carbon constraints and high facility investment costs, the construction of an internal network is not economically viable. As the carbon constraint is gradually relaxed, the network evolves from a non-facility configuration to a more dense and decentralized structure. The results also reveal a potential conflict between carbon-emission control and recycling targets. Although stricter carbon caps can effectively reduce emissions, they may simultaneously suppress recycling activities and increase the number of unrecovered batteries. Therefore, carbon-emission policies should be designed together with recycling-oriented incentives rather than implemented in isolation.

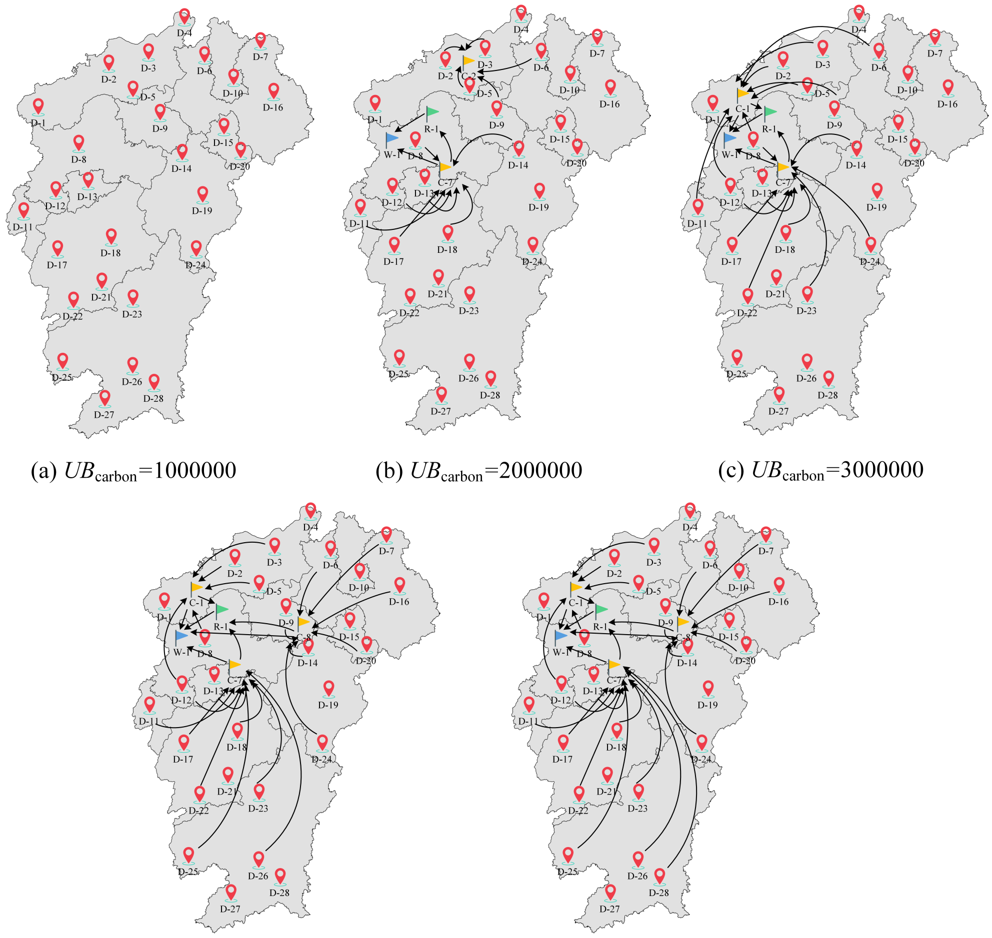

(a) UB_{carbon}=1000000 (b) UB_{carbon}=2000000 (c) UB_{carbon}=3000000

(d) UB_{carbon}=4000000 (e) UB_{carbon}=5000000

Figure 5. Spatial configuration of the EVB recycling network.

5.3.2. Impact of recovery penalty and external resource availability

To further analyze the effects of unrecovered battery penalty cost and external recycling resource availability on recycling network operations, sensitivity analysis is conducted by taking the unit penalty cost of unrecovered batteries as the key parameter under different maximum numbers of external recyclers, $Z_{\max} = 4, 5, 6$. The corresponding results are shown in Figure 6.

Figure 6(a) shows that when the penalty cost is relatively low (e.g., 1000 and 4000 USD), the internal network design cost is nearly zero, indicating that internal recycling facilities are not activated. This is because, under low penalty conditions, abandoning partial battery recovery and paying penalty costs is economically more favorable. However, when the penalty cost increases to 5660 USD and above, internal network cost increases significantly, indicating that collection centers and processing facilities are widely deployed. This result demonstrates that the penalty mechanism plays a key role in driving the system from a "recovery-avoiding" state to an "active recovery" state. Meanwhile, as $Z_{\max}$ increases, internal network cost exhibits an overall decreasing trend, suggesting that the introduction of external resources partially substitutes internal facility investment and reduces the scale of the self-built network.

Figure 6(b) shows that external recycling cost increases significantly with larger Z_{max}, since a greater number of external recyclers leads to more outsourcing of recycling tasks. It is also noteworthy that when the penalty cost is relatively high, external recycling cost tends to stabilize, indicating that the utilization of external resources gradually reaches saturation, and a relatively stable division of responsibilities between internal processing and external recycling is formed.

Figure 6(c) shows that unrecovered battery penalty cost reaches its peak at a penalty level of 4000 USD and then decreases sharply as the penalty cost further increases, eventually approaching zero. This indicates that a moderate penalty level is insufficient to fully incentivize recycling behavior, whereas a high penalty cost can significantly suppress unrecovered battery occurrences. In addition, a larger Z_{max} helps reduce the number of unrecovered batteries, especially in the medium-to-high penalty range, suggesting that external resources play an important role in alleviating insufficient internal recycling capacity.

Figure 6(d-e) show that internal recycling cost and carbon-related cost increase significantly once the penalty cost exceeds a certain threshold. This is mainly because the increase in recovered volume drives higher transportation and processing activities, thereby increasing carbon emissions and related costs. However, both types of costs decrease when Z_{max} increases because part of the recycling workload is transferred away from the self-built network. As a result, transportation and processing activities within the modeled network are reduced, leading to lower operational and carbon-emission costs within the adopted accounting boundary.

Figure 6(f) shows that total system cost increases significantly with the growth of penalty cost, which is mainly driven by simultaneous increases in internal network construction and operation expenditures, recycling costs, and carbon emission costs. However, increasing Z_{max} can effectively reduce total cost, and this reduction effect becomes more pronounced under high penalty scenarios, indicating that external resources have higher value under high-pressure conditions.

Finally, Figure 6(g-h) show that both transportation-related and processing-related carbon emissions increase significantly under high penalty cost scenarios, with processing emissions playing a dominant role. Meanwhile, a larger Z_{max} can reduce carbon emissions to some extent, suggesting that the carbon emissions generated within the self-built recycling network decrease as more recycling tasks are outsourced to external recyclers. Since the subsequent operations of external recyclers are not explicitly modeled, these results should be interpreted only within the adopted carbon-accounting boundary.

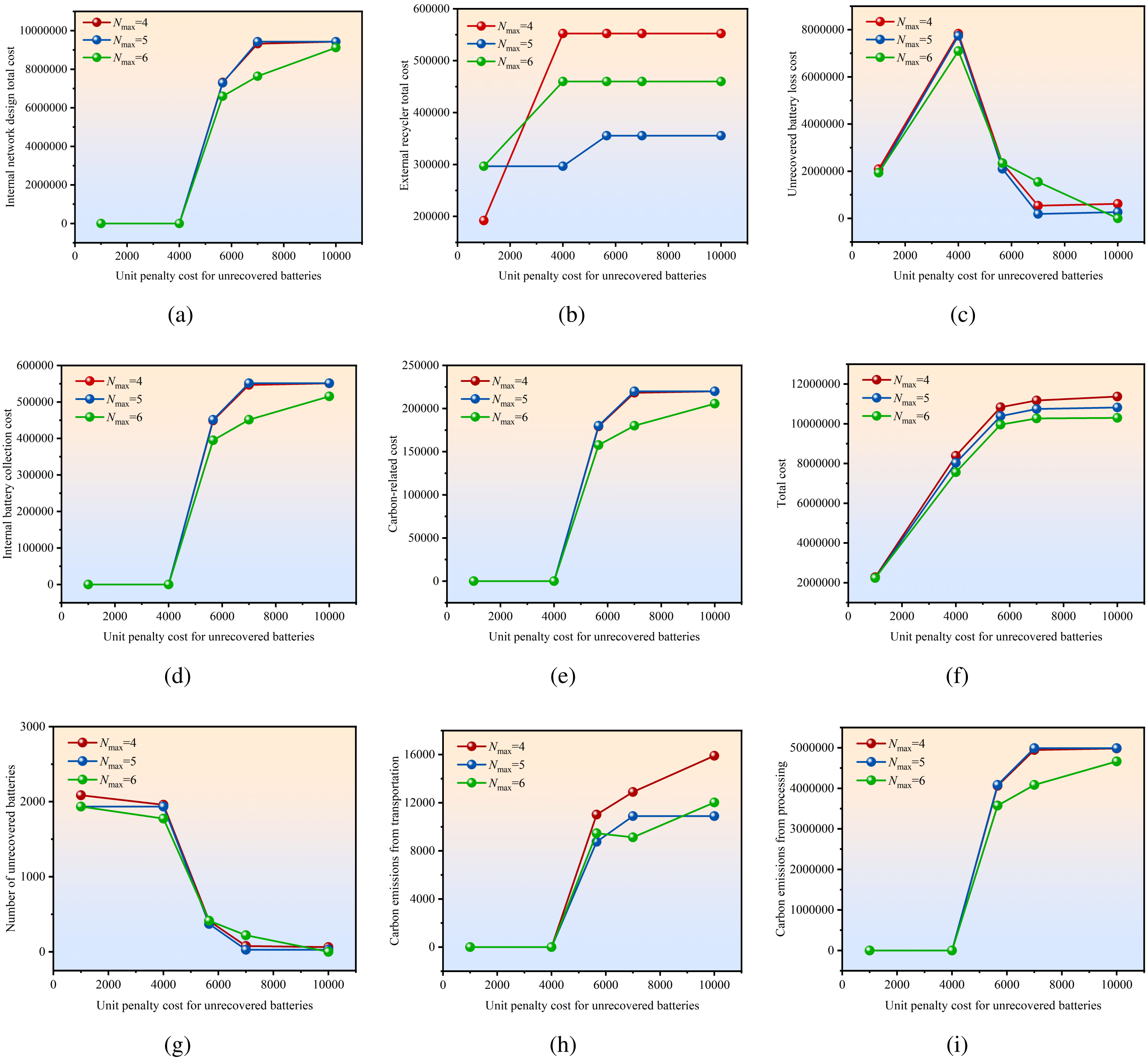

Figure 6. Impact of unit penalty cost for unrecovered batteries and maximum number of external recyclers on system performance.

In summary, the unrecovered battery penalty cost is the key driver of recycling behavior, while the scale of external recycling resources significantly affects system cost structure and operational flexibility. The interaction between these two factors leads to a trade-off relationship between internal and external resources and induces a balance between economic cost and carbon emissions. These results further suggest that recovery penalties and external resource availability should not be viewed as independent decision parameters, since their combined effects substantially influence network configuration and recycling performance. Similar observations regarding policy interaction effects and system-level adaptation have also been reported in recent studies on EVB recycling systems [45]. More broadly, Wang et al. [46] also emphasized that sustainability outcomes are jointly influenced by multiple interacting economic and policy factors.

5.3.3. Impact of combinatorial auction mechanism under carbon constraints

To analyze the impact of the combinatorial auction with WD mechanism (i.e., introduction of external recyclers) under carbon emission constraints on system performance, a comparative analysis is conducted between the cases “with external recyclers” and “without external recyclers”. The results are shown in Figure 7.

Figure 7(a) shows that, after introducing external recyclers, both internal network construction cost and operational cost decrease, while the total penalty cost of unrecovered batteries is significantly reduced. This indicates that the introduction of external recycling resources effectively enhances the overall recycling capacity of the system, thereby reducing reliance on high penalty mechanisms. Therefore, the combinatorial auction mechanism not only partially substitutes internal facility investment, but more importantly, significantly alleviates the issue of unrecovered batteries.

Figure 7(b) shows that, after introducing external recyclers, additional management costs and auction costs are incurred. However, both internal recycling cost and carbon-related cost decrease. This result indicates that part of the recycling burden is transferred from the self-built network to external recyclers, thereby reducing transportation and processing activities within the self-built network. Consequently, lower operational costs and lower carbon-emission costs are observed within the modeled network.

Figure 7(c) shows that, after introducing external recyclers, the amount of recycled batteries increases significantly, while unrecovered batteries decrease markedly, further validating the effectiveness of the combinatorial auction mechanism in improving the recovery rate. In particular, under conditions of limited internal resources, the compensatory and balancing role of external resources becomes more pronounced.

Figure 7(d) shows that transportation-related and processing-related carbon emissions within the self-built recycling network decrease after introducing external recyclers, with a more significant reduction observed in the processing stage. This result indicates that outsourcing part of the recycling tasks can reduce the transportation and processing burden borne by the internal network. Therefore, lower carbon emissions are observed within the adopted carbon-accounting boundary.

Figure 7(e) shows that total system cost decreases significantly after introducing external recyclers. This indicates that, under carbon emission constraints, the combinatorial auction mechanism can effectively improve the overall economic performance of the system and achieve coordinated optimization between cost control and recycling efficiency. In addition, significant differences in recycling routes and logistics network structures are observed under different scenarios, as illustrated in Figure 8.

In summary, under the joint effects of carbon emission constraints and disruption risks, the introduction of an external recycling mechanism based on combinatorial auctions effectively compensates for the limited capacity of the internal network and improves overall recycling efficiency. In addition, reductions in transportation and processing activities within the self-built recycling network lead to lower carbon emissions within the adopted accounting boundary. These results demonstrate the effectiveness of the proposed mechanism in improving the economic and operational performance of the recycling network under complex and uncertain environments.

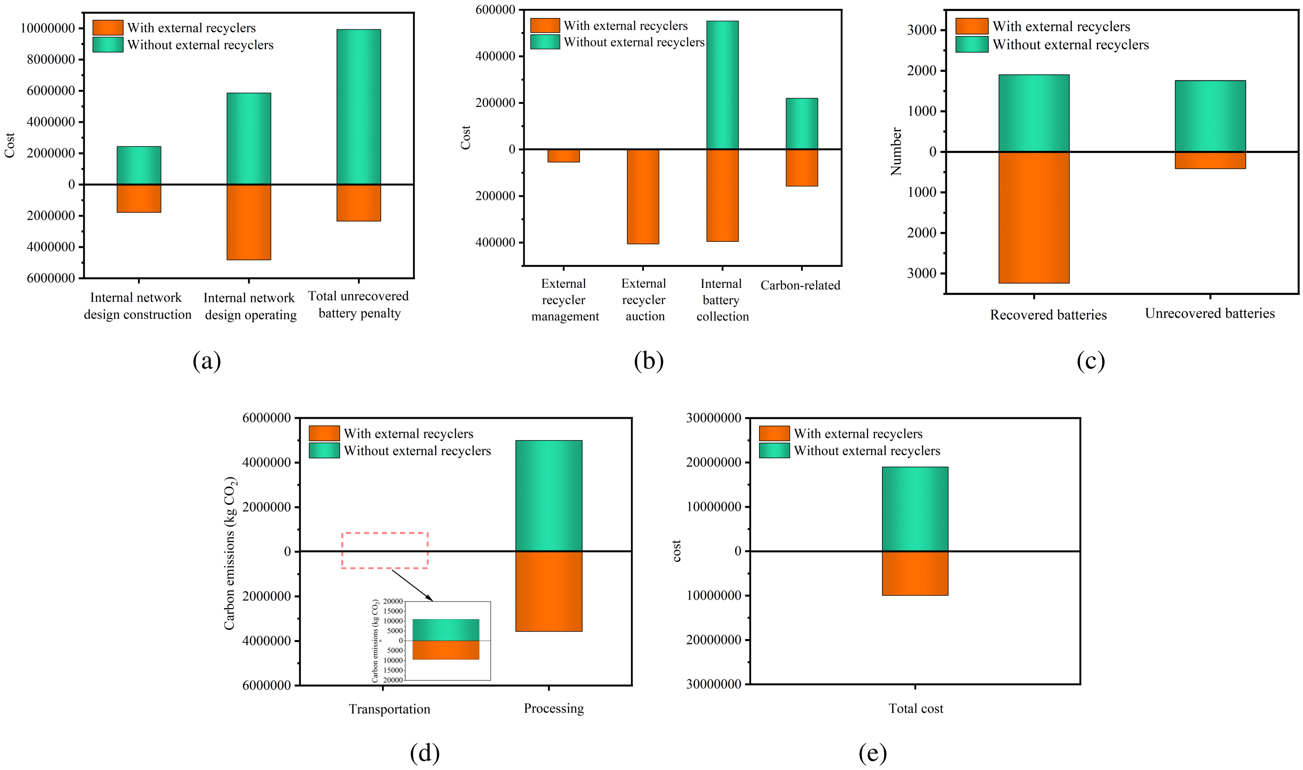

Figure 7. Impact of combinatorial auction mechanism on network performance.

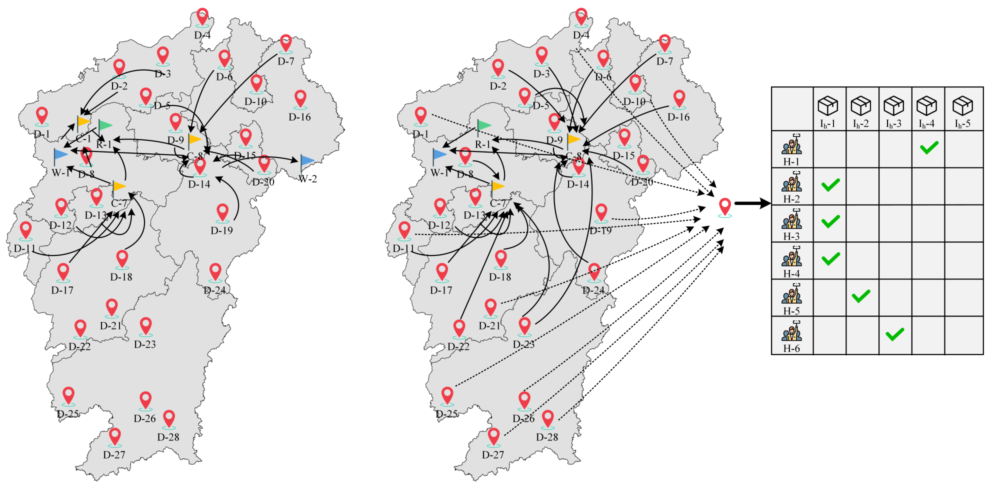

(a) With external recyclers (b) Without external recyclers

Figure 8. Spatial configuration of the EVB recycling network.

6. Managerial implications

The results indicate that carbon-emission constraints play a fundamental role in shaping recycling-network configuration and operational decisions. While stricter carbon caps can effectively reduce carbon emissions within the self-built recycling network, they may also suppress recycling activities and increase the number of unrecovered batteries. Therefore, carbon-emission policies should be designed carefully to balance environmental objectives and recycling targets, particularly in regions where battery recovery is a strategic priority.

The penalty cost of unrecovered batteries serves as an important economic driver of recycling behavior. Higher penalty levels encourage facility deployment and recycling participation, thereby reducing the quantity of unrecovered batteries. However, stronger recovery incentives may also increase transportation and processing activities. Consequently, recovery targets and environmental objectives should be coordinated rather than implemented independently.

External recyclers provide an important flexibility mechanism for coping with disruption risks and temporary capacity shortages. The results show that external resource participation can reduce system costs and improve recycling performance by alleviating the operational burden on the self-built network. In addition, the combinatorial auction mechanism enables efficient allocation of external recycling resources and enhances system adaptability under uncertain operating environments.

Overall, findings suggest that effective EVB recycling management should rely on the coordinated design of carbon-emission constraints, recovery incentives, and external resource participation. Rather than treating these factors as isolated decision instruments, decision-makers should consider their combined influence on recycling performance, economic efficiency, and system resilience. Such a coordinated approach can provide greater flexibility and robustness for EVB recycling systems operating under disruption risks and environmental regulations.

7. Conclusions

This study investigates a EVB recycling network design under green low-carbon requirements and disruption uncertainty from a 4PL coordination perspective. To address the limited adaptability of traditional recycling networks under uncertainty and the inefficiencies associated with multi-source resource allocation, the WD mechanism of combinatorial auctions is incorporated into the network design process. A two-stage stochastic programming TSSP model incorporating carbon-emission constraints is developed to jointly optimize facility location and reinforcement decisions, capacity reservation, logistics routing configuration, and external resource selection. To address the large-scale nature and computational complexity of the problem, a hybrid SR-LR algorithm that combines scenario reduction and Lagrangian relaxation is developed to improve computational efficiency. The effectiveness of the proposed model and solution approach is validated through a real-world case study and numerical experiments. The results show that carbon-emission constraints play a significant role in shaping network design decisions, substantially affecting recycling scale, cost structure, and network topology. The penalty cost of unrecovered batteries is identified as a key driver of recycling behavior, while the introduction of external recycling resources can effectively alleviate internal capacity shortages, reduce total system cost, and improve recycling efficiency. In addition, the combinatorial auction-based resource allocation mechanism captures synergies among multiple tasks, improves the efficiency of external resource selection, and enhances system flexibility and resilience under disruption scenarios. Overall, the proposed framework provides an effective balance among economic cost, recycling efficiency, and carbon-emission control, offering decision support for the design of green and resilient EVB recycling networks.

Several limitations of this study provide opportunities for future research. First, the proposed model represents disruption uncertainty through a finite set of scenarios with known occurrence probabilities. Future studies may investigate robust optimization or distributionally robust optimization when probability information is unavailable or difficult to estimate. Second, this study focuses on a single-period strategic planning problem. Extending the framework to a multi-period dynamic setting that captures the evolution of battery returns, facility capacities, and recycling demand over time would further enhance practical applicability. Third, the bidding behavior of external recyclers is assumed to be predefined and deterministic. Future research may incorporate strategic bidding and game-theoretic interactions within the combinatorial auction framework. Finally, although the proposed SR-LR algorithm demonstrates strong computational performance, integrating advanced intelligent optimization techniques, such as reinforcement learning and deep learning-assisted search, may further improve scalability and solution efficiency for large-scale stochastic recycling network design problems.

Author contributions

Yingfu Zhang: Conceptualization, methodology, formal analysis, writing–original draft; Xuefeng Wang: Conceptualization, methodology, investigation, writing–review & editing; Mingqiang Yin: Supervision, project administration, funding acquisition; Guodong Liang: Data curation; Xiaohu Qian: Resources; Chunxi Han: Visualization.

Use of Generative-AI tools declaration

The authors declare that Artificial Intelligence (AI) tools were used only for language polishing and improving the clarity of expression in this manuscript. All research ideas, model development, methodological design, numerical experiments, and result analysis were independently completed by the authors. The authors take full responsibility for the content of this manuscript.

Acknowledgments

Yingfu Zhang and Xuefeng Wang contributed equally to this work and should be considered co-first authors. This work was supported by the China Postdoctoral Science Foundation (2025MD784090); the Natural Science Foundation of Liaoning Province (2024-BS-227); the Social Science Foundation of Liaoning Province (L24CGL031); the "Xingliao Talent Program" Leading Talents Project of Liaoning Province (XLYC2402025); the National Local Joint Engineering Laboratory Project for Optimization of Petrochemical Process Operations and Energy Saving Technology of the Education Department of Liaoning Province (LJ232510148001); the Ministry of Education Humanities and Social Sciences Grant (24YJCZH231); the Guangdong Basic and Applied Basic Research Foundation Grant (2026A1515010854); the Shenzhen Philosophy and Social Science Planning Project Grant (SZ2024C013); the Foundation of Talent Scientific Research Fund of LNPU (2023XJJL-004).

Conflict of interest

The authors declare no conflict of interest.

References

1. C. Xu, Q. Dai, L. Gaines, M. Hu, A. Tukker, B. Steubing, Future material demand for automotive lithium-based batteries, *Commun. Mater.,* **1** (2020), 99. https://doi.org/10.1038/s43246-020-00095-x
2. K. Govindan, A. Jafarian, V. Nourbakhsh, Designing a sustainable supply chain network integrated with vehicle routing: a comparison of hybrid swarm intelligence metaheuristics, *Comput. Oper. Res.,* **110** (2019), 220–235. https://doi.org/10.1016/j.cor.2018.11.013
3. A. Gurtu, J. Johny, Supply chain risk management: Literature review, *Risks,* **9** (2021), 16. https://doi.org/10.3390/risks9010016
4. R. Li, X. Chen, Reverse logistics network design under disruption risk for third-party logistics providers, *Sustainability,* **14** (2022), 14936. https://doi.org/10.3390/su142214936
5. M. Huang, L. Dong, H. Kuang, Z. Z. Jiang, L. H. Lee, X. Wang, Supply chain network design considering customer psychological behavior-a 4PL perspective, *Comput. Ind. Eng.,* **159** (2021), 107484. https://doi.org/10.1016/j.cie.2021.107484
6. M. Yin, M. Huang, X. Wang, L. H. Lee, Fourth-party logistics network design under uncertainty environment, *Comput. Ind. Eng.,* **167** (2022), 108002. https://doi.org/10.1016/j.cie.2022.108002
7. M. Yin, Z. Zhang, L. Wang, X. Guo, X. Qian, M. Kamran, Optimizing sustainable and resilient electric vehicle battery recycling network: Insights from fourth-party logistics, *Sustainability,* **17** (2025), 9872. https://doi.org/10.3390/su17219872
8. C. Caplice, Y. Sheffi, Optimization-based procurement for transportation services, *J. Bus. Logist.,* **24** (2003), 109–128. https://doi.org/10.1002/j.2158-1592.2003.tb00048.x
9. X. Qian, F. T. S. Chan, M. Yin, Q. Zhang, M. Huang, X. Fu, A two-stage stochastic winner determination model integrating a hybrid mitigation strategy for transportation service procurement auctions, *Comput. Ind. Eng.*, **149** (2020), 106703. https://doi.org/10.1016/j.cie.2020.106703
10. T. Buer, R. Haass, Cooperative liner shipping network design by means of a combinatorial auction, *Flex. Serv. Manuf. J.,* **30** (2018), 686–711. https://doi.org/10.1007/s10696-017-9284-8
11. X. Wang, Q. Liu, M. Yin, Transforming electric vehicle battery recycling network with integrated winner determination for enhanced resilience, *Comput. Chem. Eng.,* (2026), 109561. https://doi.org/10.1016/j.compchemeng.2026.109561
12. L. Wang, X. Wang, W. Yang, Optimal design of electric vehicle battery recycling network–From the perspective of electric vehicle manufacturers, *Appl. Energy,* **275** (2020), 115328. https://doi.org/10.1016/j.apenergy.2020.115328
13. G. H. W. Liao, X. Luo, Collaborative reverse logistics network for electric vehicle batteries management from sustainable perspective, *J. Environ. Manage.,* **324** (2022), 116352. https://doi.org/10.1016/j.jenvman.2022.116352
14. C. Wang, X. Feng, S. Woo, J. Wood, S. Yu, The optimization of an EV decommissioned battery recycling network: A third-party approach, *J. Environ. Manage.,* **348** (2023), 119299. https://doi.org/10.1016/j.jenvman.2023.119299

15. G. Harper, R. Sommerville, E. Kendrick, L. Driscoll, P. Slater, R. Stolkin, et al., Recycling lithium-ion batteries from electric vehicles, *Nature,* **575** (2019), 75–86. https://doi.org/10.1038/s41586-019-1682-5

16. L. Gaines, The future of automotive lithium-ion battery recycling: Charting a sustainable course, *Sustain. Mater. Technol.,* **1** (2014), 2–7. https://doi.org/10.1016/j.susmat.2014.10.001

17. J. B. Dunn, L. Gaines, J. C. Kelly, C. James, K. G. Gallagher, The significance of Li-ion batteries in electric vehicle life-cycle energy and emissions and recycling's role in its reduction, *Energy Environ. Sci.,* **8** (2015), 158–168. https://doi.org/10.1039/C4EE03029J

18. K. Govindan, H. Soleimani, D. Kannan, Reverse logistics and closed-loop supply chain: A comprehensive review to explore the future, *Eur. J. Oper. Res.,* **240** (2015), 603–626. https://doi.org/10.1016/j.ejor.2014.07.012

19. M. T. Melo, S. Nickel, F. Saldanha-Da-Gama, Facility location and supply chain management–A review, *Eur. J. Oper. Res.,* **196** (2009), 401–412. https://doi.org/10.1016/j.ejor.2008.05.007

20. R. Z. Farahani, M. SteadieSeifi, N. Asgari, Multiple criteria facility location problems: A survey, *Appl. Math. Model.,* **34** (2010), 1689–1709. https://doi.org/10.1016/j.apm.2009.10.005

21. C. S. ReVelle, H. A. Eiselt, Location analysis: A synthesis and survey, *Eur. J. Oper. Res.,* **165** (2005), 1–19. https://doi.org/10.1016/j.ejor.2003.11.032

22. H. Min, H. J. Ko, The dynamic design of a reverse logistics network from the perspective of third-party logistics service providers, *Int. J. Prod. Econ.,* **113** (2008), 176–192. https://doi.org/10.1016/j.ijpe.2007.01.017

23. M. S. Pishvaee, J. Razmi, S. A. Torabi, An accelerated Benders decomposition algorithm for sustainable supply chain network design under uncertainty: A case study of medical needle and syringe supply chain, *Transp. Res. Part E,* **67** (2014), 14–38. https://doi.org/10.1016/j.tre.2014.04.001

24. L. C. Casals, B. A. García, C. Canal, Second life batteries lifespan: Rest of useful life and environmental analysis, *J. Environ. Manage.,* **232** (2019), 354–363. https://doi.org/10.1016/j.jenvman.2018.11.046

25. Q. Tan, J. Li, L. Yang, G. Xu, Cascade use potential of retired traction batteries for renewable energy storage in China under carbon peak vision, *J. Clean. Prod.,* **412** (2023), 137379. https://doi.org/10.1016/j.jclepro.2023.137379

26. L. V. Snyder, Facility location under uncertainty: A review, *IIE Trans.,* **38** (2006), 547–564. https://doi.org/10.1080/07408170500216480

27. W. Yan, X. Wang, Y. Liu, X. M. Zhang, Z. G. Jiang, L. Huang, A stochastic programming approach for EOL electric vehicle batteries recovery network design under uncertain conditions, *Sci. Rep.,* **14** (2024), 876. https://doi.org/10.1038/s41598-024-51169-6

28. S. Rosenberg, S. Huster, A. Rudi, F. Schultmann, Assessing economic uncertainty in dynamic reverse logistics networks- A stochastic modeling approach for planning circular battery treatment, *Comput. Ind. Eng.,* **201** (2025), 110900. https://doi.org/10.1016/j.cie.2025.110900

29. A. Win, The value a 4PL provider can contribute to an organisation, *Int. J. Phys. Distrib. Logist. Manage.,* **38** (2008), 674–684. https://doi.org/10.1108/09600030810925962

30. M. Hingley, A. Lindgreen, D. B. Grant, C. Kane, Using fourth-party logistics management to improve horizontal collaboration among grocery retailers, *Supply Chain Manag.,* **16** (2011), 316–327. https://doi.org/10.1108/13598541111155839

31. Y. Tao, E. P. Chew, L. H. Lee, Y. Shi, A column generation approach for the route planning problem in fourth party logistics, *J. Oper. Res. Soc.,* **68** (2017), 165–181. https://doi.org/10.1057/s41274-016-0024-3

32. S. de Vries, R. V. Vohra, Combinatorial auctions: A survey, *INFORMS J. Comput.,* **15** (2003), 284–309. https://doi.org/10.1287/ijoc.15.3.284.16077

33. N. Li, Y. Zhang, S. Tiwari, G. Kou, Winner determination problem with purchase budget for transportation procurement under uncertain shipment volume, *Transp. Res. Part E,* **176** (2023), 103182. https://doi.org/10.1016/j.tre.2023.103182

34. C. Triki, M. R. Hasan, A. Elomri, Solving the winner determination problem with discounted bids in transportation auctions, *Ann. Oper. Res.,* **351** (2025), 35–58. https://doi.org/10.1007/s10479-023-05457-5

35. T. Bektaş, G. Laporte, The Pollution-Routing Problem, *Transp. Res. Part B,* **45** (2011), 1232–1250. https://doi.org/10.1016/j.trb.2011.02.004

36. A. Chaabane, A. Ramudhin, M. Paquet, Design of sustainable supply chains under the emission trading scheme, *Int. J. Prod. Econ.,* **135** (2012), 37–49. https://doi.org/10.1016/j.ijpe.2010.10.025

37. Z. Wang, B. Zhang, D. Guan, Take responsibility for electronic-waste disposal, *Nature,* **536** (2016), 23–25. https://doi.org/10.1038/536023a

38. J. Li, F. Liu, J. Z. Zhang, Z. Tong, Optimal configuration of electric vehicle battery recycling system under across-network cooperation, *Appl. Energy,* **338** (2023), 120898. https://doi.org/10.1016/j.apenergy.2023.120898

39. M. He, Q. Li, X. Wu, K. Izui, Designing a multi-level reverse logistics network for waste batteries of electric vehicles under uncertainty–A case study in the Yangtze River Delta Urban Agglomerations of China, *J. Clean. Prod.,* **472** (2024), 143418. https://doi.org/10.1016/j.jclepro.2024.143418

40. L. V. Snyder, M. S. Daskin, Models for reliable supply chain network design, In: *Critical Infrastructure,* Springer, Berlin, Heidelberg, 2007. https://doi.org/10.1007/978-3-540-68056-7_13

41. R. Karuppiah, M. Martin, I. E. Grossmann, A simple heuristic for reducing the number of scenarios in two-stage stochastic programming, *Comput. Chem. Eng.,* **34** (2010), 1246–1255. https://doi.org/10.1016/j.compchemeng.2009.10.009

42. M. Yin, M. Huang, D. Wang, S. C. Fang, X. Qian, X. Wang, Multi-period fourth-party logistics network design with the temporary outsourcing service under demand uncertainty, *Comput. Oper. Res.,* **164** (2024), 106564. https://doi.org/10.1016/j.cor.2024.106564

43. M. Yin, Y. Zhou, X. Qian, Q. Liu, X. Guo, Optimizing multi-period green electric vehicle battery recycling network: Integrating winner determination within a 4PL framework, *IEEE Trans. Eng. Manag.,* **73** (2026), 1769–1783. https://doi.org/10.1109/TEM.2026.3658193

44. Z. Wang, Z. Zhang, M. Yin, N. Yuan, X. Qian, X. Li, 4PL-driven optimization of electric vehicle battery recycling networks: Enhancing greenness, timeliness and resilience against disruptions, *Waste Manag.,* **222** (2026), 115650. https://doi.org/10.1016/j.wasman.2026.115650

45. H. Zhang, Y. Wang, H. Liu, R. Chen, Optimizing policy mix for circular technology transitions: A networked co-evolution framework for electric vehicle battery recycling, *J. Clean. Prod.,* **555** (2026), 148183. https://doi.org/10.1016/j.jclepro.2026.148183

46. Y. Wang, Y. Shi, X.-M. Zhou, S.-Y. Li, Z.-M. Sun, X.-C. Xia, et al., Sustainability analysis: Research on China's real estate economy and business based on the CFPS data, *Sustainability,* **18** (2026), 3278. https://doi.org/10.3390/su18073278